Public

Report

Document ID	Version	Status	Reg no	Page
1193244	4.0	Approved		1 (65)
Author: Lennart Agrenius			Date: 2009-12-10	
Reviewed by			Reviewed date	
Approved by: Olle Olsson			Approved date: 2010-12-16	
Comment: Reviewed SKBdoc 1202026				

Criticality safety calculations of disposal canisters

Summary

In the planned Swedish repository for disposal of spent nuclear fuel (SNF) the fuel assemblies will be placed in disposal canisters made of cast iron and copper.

To assure safe disposal of the SNF, one requirement is that the normal criticality safety criteria have to be met. The effective neutron multiplication factor must not exceed 0.95 in the most reactive conditions when the canister is filled with water, including different kinds of uncertainties. In this report it is shown that the criteria could be met if credit for the reactivity decrease due to the burnup of the fuel is taken into account for all fuel types including MOX-fuel.

Record of changes

Ver	Change	Author	Date	Reviewed	Approved
1.0	Revised report according to SKBdoc 1202026.	Lennart Agrenius	2009-12-10	See header	See header
2.0	Changed fig 14, 15, 16 and 17 and table 27, 28 and 41 to U-235. Changed in fig 10, 11 and fig 42, 43, 44, 45 from U235 to U-235.	Lennart Agrenius	2010-05-18		
3.0	Reference 6, 19, 23, 24 and 25 are added in SKBdoc. 19, 23, 24 and 25 as links.	Per H Grahn	2010-08-20		See header
4.0	Editorial changes in the text. Reference list revised.	Per H Grahn	2010-12-06		See header

Table of Contents

1 Introduction

In the planned Swedish repository for disposal of spent nuclear fuel (SNF) the fuel assemblies will be placed in disposal canisters made of cast iron and copper.

To assure safe disposal of the SNF, one requirement is that the normal criticality safety criteria have to be met. The effective neutron multiplication factor must not exceed 0.95 in the most reactive conditions when the canister is filled with water, including different kinds of uncertainties.

Earlier calculations show that the effective neutron multiplication factor exceeds 0.95 if fresh fuel is assumed /1/. Earlier calculations also show that the criticality criteria could be met if burnup credit is used /2/. In this report these calculations are updated and it is shown that the criteria could be met if credit for the reactivity decrease due to the burnup of the fuel is taken into account.

2 Objective

The purpose with this study is to assess the disposal canister regarding criticality and the use of burnup credit to keep the $k_{eff} < 0.95$ when the disposal canister is filled with water.

3 Methods

All calculations were performed using Scale 5.1 /3/. Depletion calculations were performed using the Scale SAS2 control sequence and the criticality calculations were performed using Starbucs and CSAS25. The calculations were performed using the Scale 44-group ENDF/B-V library.

The SAS2 control module was originally developed for SCALE to provide a sequence that generated radiation source terms for spent fuel and subsequently utilized these sources within a one-dimensional (1-D) radial shielding analysis of a shipping cask. For each time-dependent fuel composition, SAS2 performs 1-D neutron transport analyses (via XSDRNPM) of the reactor fuel assembly using a two-part procedure with two separate lattice-cell models. The first model is a unit fuel-pin cell from which cell-weighted cross sections are obtained. The second model represents a larger unit cell (e.g., an assembly) within an infinite lattice. The larger unit-cell zones can be structured for different types of BWR or PWR assemblies containing water holes, burnable poison rods, gadolinium fuel rods, etc. The (fuel) neutron flux spectrum obtained from the second (large) unit-cell model is used to determine the appropriate nuclide cross sections for the specified burnup-dependent fuel composition. The cross sections derived from a transport analysis at each time step are used in a point-depletion computation (via ORIGEN-S) that produces the burnup-dependent fuel cross section libraries to be used in the next spectrum calculation. This sequence is repeated over the operating history of the reactor.

In Starbucs burnup calculations are made for several axial zones in a fuel assembly. Cross sections are generated as input to a 3D Keno Va-model.

It should be noted that a result from Keno Va (normally k_{eff}) is associated with a statistical uncertainty, which has to be considered when comparing the results from two calculations. No of neutrons per generation is 5000 and number of neutrons per generation is 3000.

If a change in a parameter in the model gives a difference in k_{eff} smaller than the statistical spread (2σ) the difference is caused by the statistical uncertainty and not by the parameter change.

4 Criticality safety criteria

The criticality safety criteria are based on the US NRC regulatory requirements for transportation and storage of spent fuel. The US NRC positions are found in several regulatory guides:

Regulatory guide 3.58 – Criticality Safety Criteria for the Handling, Storing and Transporting LWR Fuel at Fuels and Materials Facilities

Regulatory guide 1.13 – Proposed revision 2 to Regulatory Guide 1.13 Spent Fuel Storage Facility

NRC issued revision 2 of ISG 8 which gives recommendations concerning burnup credit of PWR fuel.

FCSS-ISG-10 revision 2 concerns the minimum margin of subcriticality for safety of fuel cycle facilities.

The basic criticality criteria is that the effective neutron multiplication factor should not exceed 0.95 including uncertainties and the nuclear safety analysis should include considerations of all credible normal and abnormal operating occurrences. Credit for fuel burnup may be taken.

5 Description of the system

5.1 Disposal Canister

A disposal canister consists of an insert of cast iron with a diameter of 949 mm with a 49 mm thick outer shell of copper. The outside diameter of a disposal canister is 1050 mm. During the casting process compartments for the fuel assemblies' storage positions are formed by square-formed tubes of steel. The wall thicknesses of these tubes are 10 mm for the BWR-case and 12.5 mm for the PWR-case. In the BWR-insert twelve storage compartments are formed with the inner measures of 160 mm x 160 mm. In the PWR-insert four storage compartments are formed with the inner measures of 235 mm x 235 mm.

BWR radial section PWR radial section

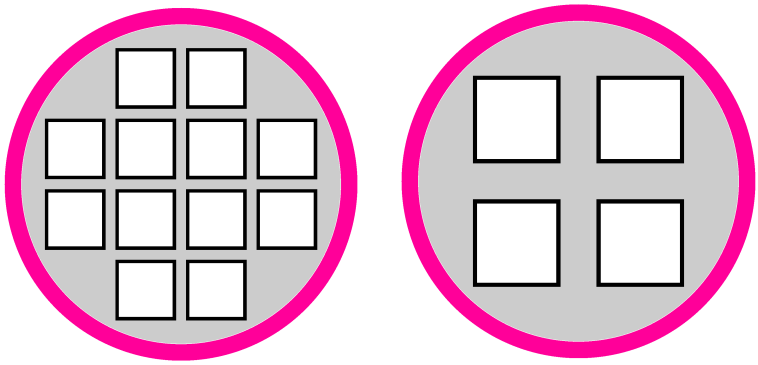

BWR axial section

PWR axial section

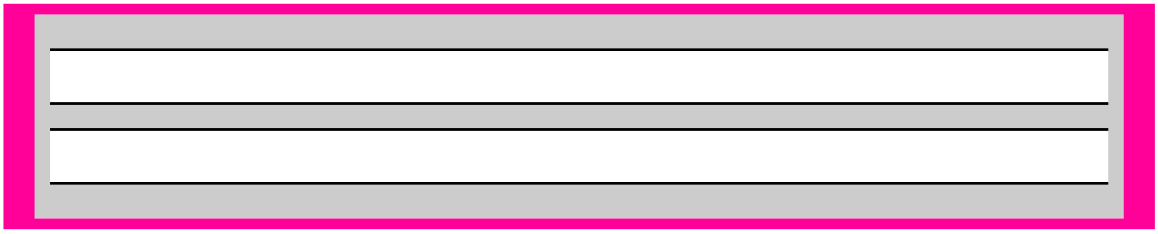

Figure 1 – Cross sections of the BWR- and PWR-disposal canister.

In table 1 the main parameters of the disposal canisters are presented /4/.

Table 1 – Main parameters for the disposal canisters

Parameter	BWR		PWR	
	Value	Tolerances	Value	Tolerances
No positions	12		4	
C-C distance between compartments (mm)	210	+1/-4	370	±3.6
Compartment size, outer (mm)	180	±1.8	260	±2.6
Compartment tube wall thickness (mm)	10	±1.0	12.5	±1.25
Compartment size, inner (mm)	160	±3.8 Note	235	±5.1 Note
Insert diameter (mm)	949	+0.5/-0.0	949	+0.5/-0.0
Shell inner diameter (mm)	952	±0.5	952	±0.5
Shell outer diameter (mm)	1050	±1.2	1050	±1.2
Shell thickness (mm)	49	±0.3	49	±0.3
Insert material	Nodular Cast Iron	-	Nodular Cast Iron	-
Insert material density (kg/dm^3)	7.1	-	7.1	-
Tube material	Steel	-	Steel	-
Tube material density (kg/dm^3)	7.85	-	7.85	-
Insert lid material	Steel		Steel	
Insert lid material density (kg/dm^3)	7.85		7.85	
Shell material	Cu	-	Cu	-
Copper density (kg/dm^3)	8.9	-	8.9	-
Length of compartment (mm)	4463	+5/-10	4443	+5/-10
Length of insert (mm)	4573	+0/-0.5	4573	+0/-0.5
Length of canister (incl. Cu shell)	4835	+3.25/-2.75	4835	+3.25/-2.75

Note. The tolerance in the inner compartment size is a combination of the tolerances in the compartment outer size and in compartment tube wall thickness.

5.2 Materials in the disposal canister

The insert consists of nodular cast iron (SS 140717), the tubes forming the compartments of steel (S355J2H) and the insert lid of steel (S355J2). The compositions are shown in table 2, 3 and 4.

Table 2 – SS 140717

Material	C	Si	Mn	P	S	Ni	Mg
Min (%)	3.2	1.5	0.05	-	-	0	0.02
Max (%)	4	2.8	1	0.08	0.02	2	0.08

Fe-content 90.02 - 95.13% (balance)
Density 7.1 g/cm^3

Table 3 – S355J2H

Material	C	Si	Mn	P	S
Max (%)	0.22	0.55	1.6	0.03	0.03

Fe-content 97.57% (balance)
Density 7.85 g/cm^3

Table 4 – S355J2

Material	C	Si	Mn	P	S	Cu
Max (%)	0.24	0.6	1.7	0.035	0.035	0.6

Fe-content 96.79% (balance)
Density 7.85 g/cm^3

The disposal canister shell is made of pure copper, density 8.9 g/cm^3.

In the repository the disposal canister is surrounded by a 35 cm layer of bentonite with the composition according to table 5.

Table 5 – Bentonite

Material	Al	Fe	Mg	Si	O	H	Na	Ca	K	C	S
Share (%)	8.91	1.86	0.97	24.99	57.89	2.56	0.95	0.58	0.79	0.45	0.05

Density 2.05 g/cm^3

The composition of the bentonite is from /5/.

Table 6 – Continental earth crust

Material	Si	O	Mg	K	Fe	Ca	Al	Na	Mn	S	C
Share (%)	30.6	46.8	1.3	2.7	3.3	3	7.9	2.7	0.6	0.6	0.6

Density 2.5 g/cm^3.

The rock between the disposal canisters is modeled as “continental earth crust” with the composition according to table 6 from /SKBdoc 1251579, ver 1.0/.

5.3 Fuel types

In the Swedish program the existing and planned main fuel types are:

The maximum enrichment is 5% U-235 and the maximum burnup is 60 MWd/kgU for both BWR and PWR.The maximum burnup for Atrium10B MOX is 50 MWd/kg HM.

BWR-fuel types

AA 8x8, Exxon 8x8, KWU 8x8-2,

ANF 9x9-5, KU 9x9-5, KWU 9x9-Q, Atrium 9A/B,

Atrium 10B, Atrium 10 MOX, Atrium 10XM, GE11S, GE12S, GE14, GNF2,

Svea 64,

Svea 100,

Svea 96, Svea 96, Optima, Svea 96 Optima 2 and Svea 96 Optima 3.

Data for the BWR fuel types are given in Appendix 2.

MOX-fuel is Atrium 10B and contains 4.6% Pu_{fiss} and 0.2% U-235.

PWR- fuel types

W15x15, KWU15x15, F15x15AFA3G, 15x15AGORA,

W17x17, AA17x17, F17x17, S17x17HTP, 17x17 HTP, 17x17 HTP M5, 17x17 HTP M5 monobloc, 17x17 AFA3G.

Data for the PWR fuel types are given in Appendix 3.

5.4 Irradiation history of the fuel assemblies

In order to calculate the isotopic composition of the fuel at different burnup the fuel had to be subjected to different burnup histories. The main parameters for the depletion calculation are shown in table 7.

The burnup of a fuel assembly is always the assembly average burnup if nothing else is stated.

Table 7 – Main parameters for the depletion calculation

Parameter	BWR	PWR
Assembly power (MW)	4	15
Avg. fuel temperature (°C)	584	625
Coolant pressure (bar)	70	155
Coolant temperature (°C)	286	304
Boron concentration (ppm)	-	600
Coolant density (kg/dm^3)	0.33	0.68
Cycle length (days)	345	345
Shutdown length (days)	20	20
Decay time (yrs)	1	1

(Sources: Ringhals 2007-10-19, 1960160/1.1 and OKG 2008-05-26, reg nr 2008-14670. Confidential information. Available only for the Swedish Radiation Safety Authority.)

The depletion parameters are further discussed in section 8.

6 Analysis

6.1 Analysis for selection of design case

In criticality calculations it is common practice to use the most reactive configuration.
In this section variations of different parameters were investigated in order to find the most reactive configuration. The resulting configuration, called “the design case”, was used as basis for the burnup credit loading curves for the disposal canister.

The nominal calculation geometry of the disposal canister was:

Nominal c-c distance between compartments (BWR 210 mm, PWR 370 mm)

Nominal compartment size (BWR 160 mm, PWR 235 mm)

Nominal insert diameter (949 mm)

Maximum Fe content in the insert steel (95%)

Nominal compartment tube wall thickness (BWR 10 mm, PWR 12.5 mm)

Nominal copper shell inner diameter (952 mm)

Nominal copper shell thickness (49 mm)

Nominal compartment length (BWR 4463 mm, PWR 4443 mm)

Nominal insert length (4573 mm)

Nominal length of copper disposal canister (4835 mm)

The disposal canister is located in the final repository surrounded by bentonite (350 mm thick)

Bentonite on top and bottom of the disposal canister (350 mm)

Assemblies are located at the centre of the compartments
Compartments are filled with water
Gap between insert and copper shell is modeled as water

The temperature is 293 K

The model is in three dimensions. The calculations were performed with fresh fuel with an initial enrichment of 5% U-235.

The following parameters were analyzed:

- Fuel type
- Material compositions
- Location of the disposal canister
- Position of the fuel assemblies in the disposal canister
- Disposal canister manufacturing tolerances
- Temperature

6.2 Fuel types

Criticality calculations were performed for all fuel types in appendix 2 and 3 assuming fresh fuel. Burnable poison is not modeled. The average enrichment is 5% U-235. All axial sections with regard to part length rods are included in the analysis. For Svea 96 Optima 3 the bottom zone with 96 fuel rods is used in the analysis.

The purpose was to determine which fuel type that is most reactive in the disposal canister, the resulting k_{eff} are shown in table 8.

Table 8 – k_{eff} for different fuel types (σ=0.0002)

Fuel type	k_{eff}
W15x15	1.0852
KWU15x15	1.0844
F15*15AFA3G	**1.0888**
15x15AGORA	1.0878
W17x17	1.0855
AA17*17	1.0853
F17*17	1.0856
S17*17 HTP	1.0825
17x17 HTP	1.0828
17x17 HTP M5	1.0862
17x17 HTP M5 monobloc	1.0856
17x17 AFA3G	1.0853
AA 8x8	0.9569
Exxon 8x8	0.9509
KWU 8x8-2	0.9635
ANF 9x9-5	0.9705
KWU 9x9-5	0.9716
KWU 9x9-Q	0.9661
Atrium 9A/B	0.9726
Atrium 10B	0.9738
Atrium 10 XM	0.9743
Atrium 10 MOX	0.9038
GE11S	0.9709
GE12S	0.9779
GE14	0.9741
GNF2	0.9686
Svea 64	0.9814
Svea 100	0.9879
Svea 96	0.9881
Svea 96 Optima	0.9849
Svea 96 Optima 2	0.9889
Svea 96 Optima 3	**0.9959**

It can be seen that the most reactive fuel assembly type in disposal canister geometry is F15x15AFA3G for PWR and Svea 96 Optima 3 for BWR. These fuel types cover all fuel types including MOX-fuel and will be used as reference fuel types in this study.

To check if there is a burnup dependence of the reactivity difference k_{eff} was also calculated as function of burn up for the BWR-fuel types and for F15x15AFA3G and F17x17. The result is presented in figures 2 and 3.

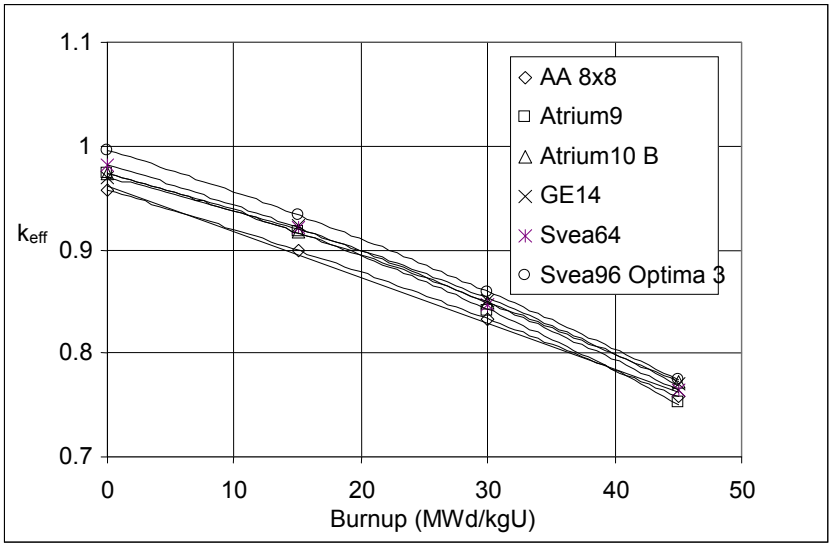

Figure 2 – k_{eff} of BWR- fuel assemblies.

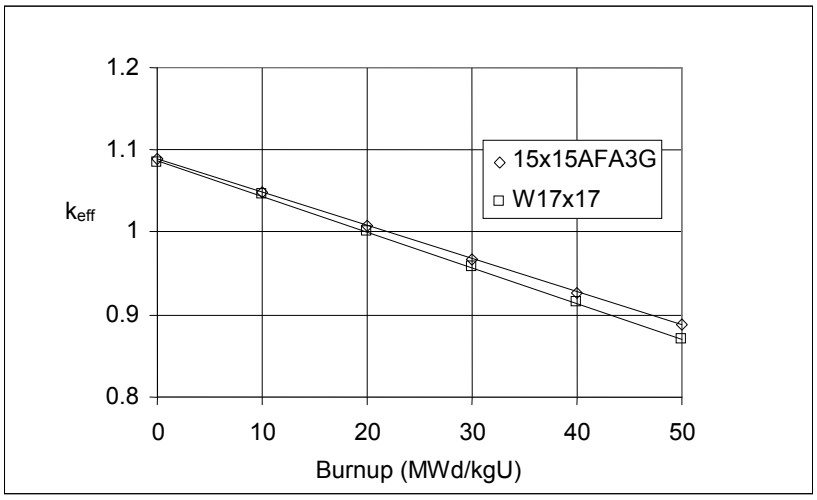

Figure 3 – k_{eff} of PWR- fuel assemblies.

It can be seen that Svea 96 Optima 3 is the most reactive BWR-fuel and F15x15AFA3G is the most reactive PWR-fuel type over the whole burnup range.

6.3 Material composition

6.3.1 Nodular cast iron

The Fe-content in the nodular cast iron in the disposal canister insert could vary between 90% and 95% according to the specification in table 2.

In order to analyze the sensitivity of the composition of nodular cast iron calculations were made for the nodular cast iron compositions in table 2. The disposal canister geometry was as described in section 6.1 except for the nodular cast iron composition, which was varied. The results are shown in table 9 and figure 4 for PWR and BWR

Table 9 – k_{eff} for different nodular iron composition (σ=0.0002)

Material composition			k_{eff}	
Iron	**Carbon**	**Silicon**	**PWR**	**BWR**
0.9000	0.0600	0.4000	1.0898	0.9974
0.9223	0.0474	0.0303	1.0880	0.9968
0.9423	0.0374	0.0203	1.0887	0.9955
0.9623	0.0274	0.0103	1.0886	0.9951
0.9823	0.0174	0.0003	1.0878	0.9938

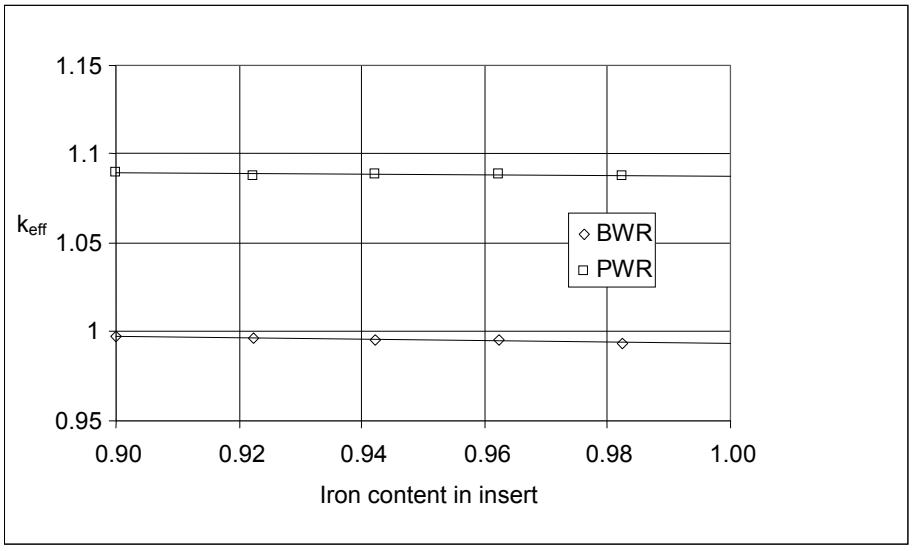

Figure 4 – k_{eff} as function of iron content in the insert.

It is seen that the reactivity increases if the iron content is decreased. The reason for this is the iron is replaced by carbon and silicon. These materials contribute to the reactivity.

In order to cover possible compositions of the nodular cast iron the following composition is used in the design case: Iron 0.9, Carbon 0.06 and Silicon 0.04. With this assumption the criticality analysis covers nodular cast iron with compositions: Iron >0.9, Carbon <0.06 and Silicon <0.04.

6.3.2 Density in the insert

The nominal density of nodular cast iron is 7.1 kg/dm^3. The influence of variations of this density was investigated. The disposal canister geometry was as described in section 6.1 except for the nodular cast iron density, which was varied. The results are shown in figure 5.

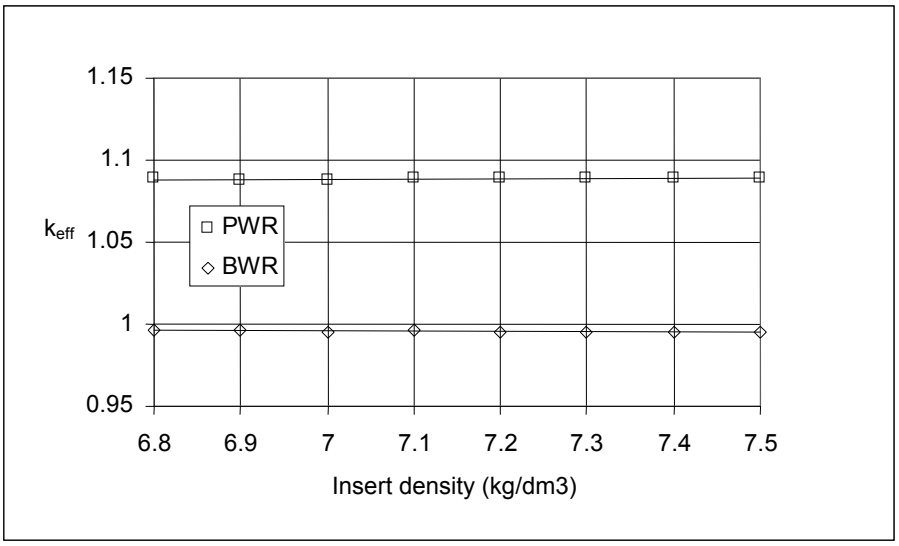

Figure 5 – k_{eff} as function of density in the insert.

It can be seen that the reactivity is relatively independent on the insert density. A slight increase of k_{eff} with increasing density can be seen in the PWR-case and a slight decrease in the BWR-case. In order to cover possible variation in the nodular cast iron density 7.3 kg/dm^3 is used for the PWR-case and 6.9 kg/dm^3 for the BWR-case in the design model.

6.3.3 Steel in the compartment tube walls

Variations in the steel composition in the compartment tube walls and the lid were investigated. Three cases were investigated, see table 10.

Table 10 - k_{eff} for different steel composition in the compartment tube walls (σ=0.0002)

Case	Fraction of						k_{eff}	
	Iron	Carbon	Silicon	Manganese	Phosphorus	Sulfur	PWR	BWR
1	0.9600	0.0100	0.0134	0.0160	0.0003	0.0003	1.0886	0.9963
2	0.9757	0.0022	0.0055	0.0160	0.0003	0.0003	1.0888	0.9959
3	0.9800	0.0001	0.0034	0.0160	0.0003	0.0003	1.0886	0.9953

It can be seen that case 1 with the lowest iron content gives the highest reactivity for BWR-case. For the PWR-case no significant change in k_{eff} is observed.

In order to cover possible compositions of the steel in the tube walls the composition according case 1 is used in the design case. With this assumption the criticality analysis covers steel with compositions: Iron > 0.96, Carbon <0.01 and Silicon <0.013.

6.3.4 Density in compartment tube walls

The nominal density of the steel in the compartment tube walls is 7.85 kg/dm^3. The influence of variations of this density was investigated. The disposal canister geometry was as described in section 6.1 except for the nodular cast iron density, which was varied. The results are shown in figure 6.

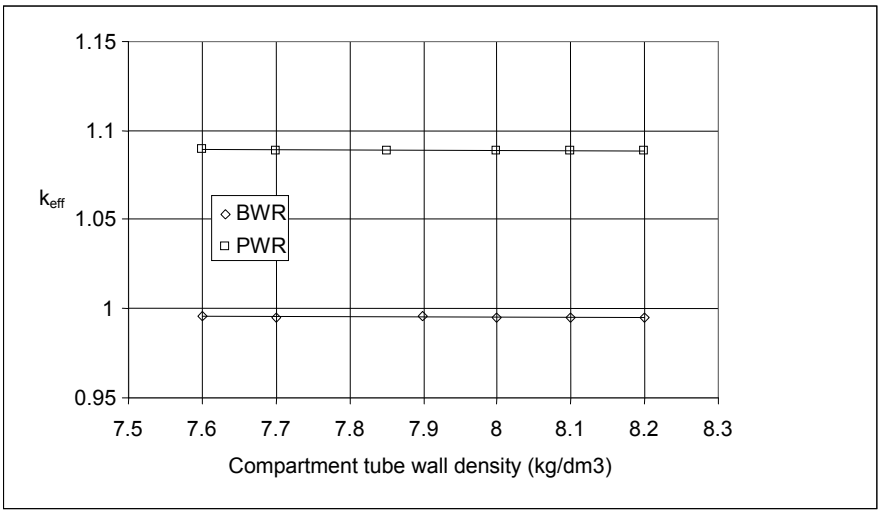

Figure 6 – k_{eff} as function of density in the tube walls.

A small reactivity decrease with increasing density can be seen. In order to cover possible variation in the steel in the tube walls the density 7.7 kg/dm^3 is used in the design model.

6.3.5 Bentonite

Variations in bentonite composition give small or no changes in the reactivity of the disposal canister.

6.3.6 Earth crust

Variations in earth crust (rock) composition give small or no changes in the reactivity of the disposal canister.

6.4 Location of the disposal canister

The objective with this section is to identify the most reactive location of the disposal canister.

6.4.1 Encapsulation plant

In the encapsulation plant the disposal canisters are loaded with fuel assemblies in dry conditions. The worst situation from a criticality standpoint occurs if the disposal canister is filled with water during this process. Two situations could occur.

1. The disposal canister is filled with water. The rest of the surrounding space is dry. Neutrons leaking from the disposal canister could be reflected back to the disposal canister by the concrete in the walls of the room.

   PWR:$k_{eff}\pm\sigma$= 1.0860±0.0002

   BWR:$k_{eff}\pm\sigma$= 0.9926±0.0002

2. Both the disposal canister and the surrounding space are filled with water. Neutrons leaking from the disposal canister could be reflected back to the disposal canister by the water.

   PWR:$k_{eff}\pm\sigma$ = 1.0872±0.0002

   BWR: $k_{eff}\pm\sigma$ = 0.9942±0.0002

6.4.2 Storage room

After the disposal canister is loaded with fuel assemblies, it is filled with argon and the disposal canister lid is welded on the disposal canister. The disposal canister is put in a transport cask and transported to a storage room. k_{eff} is less than 0.4 for both PWR- and BWR-case for an infinite number of disposal canisters in transport casks.

6.4.3 Transport

From the storage location the disposal canisters are transported in a transport cask to the repository.

During transport the disposal canister is protected by the transport cask, which presently is being developed. A preliminary design of such a cask was done. (Source: SKBdoc 1038365, ver 1.0. Confidential information. Available only for the Swedish Radiation Safety Authority.) This preliminary cask consists of a cylindrical steel container. The inside diameter is 106 cm and the steel thickness is 16 cm with 8 cm neutron shielding outside. The neutron shielding is made of resin compound, which is a plastic material.

In normal conditions the disposal canister is leak tight and the atmosphere in the disposal canister is dry argon. In this case with no water present the effective neutron multiplication factor is less than 0.4 and the system is indeed sub critical.

The worst situation from a reactivity standpoint will occur in an accident situation if the transport cask and disposal canister are damaged, the cask is submerged in water and both the cask and disposal canister are filled with water.

In this case the $k_{eff}\pm\sigma$=1.0952 ± 0.0002 for PWR and $k_{eff}\pm\sigma$ =1.0012± 0.0002 for BWR.

The canister-cask is a double barrier system and it is presently not clear if this situation needs to be considered.

6.4.4 Disposal

At the repository the disposal canister is deposited in the rock. The disposal canister is surrounded by 35 cm thick rings of bentonite. After some years it is assumed that water has leaked into and filled the disposal canister.

A disposal canister deposited in the repository surrounded by 35 cm bentonite and filled with water gives $k_{eff}\pm\sigma$=1.0888±0.0002 for PWR and $k_{eff}\pm\sigma$= 0.9959 ±0.0002 for BWR.

To study the effect of interaction between deposited disposal canisters in the repository an infinite number of disposal canisters were modeled with centre to centre distance of 6 m. The disposal canisters were surrounded by 35 cm bentonite and the space between the disposal canisters was modeled as rock according to table 6.

$k_{eff}\pm\sigma$= 1.0886±0.0002 for PWR and $k_{eff}\pm\sigma$=0.9951 ±0.0002 for BWR.

The results show that the interaction between disposal canisters is insignificant.

6.4.5 Summary

The results are summarized in table 11.

Table 11 – k_{eff} at different locations (σ=0.0005)

Situation	k_{eff}	
	BWR	**PWR**
Accident in the encapsulation process area	0.9942	1.0872
Storage of several disposal canisters	< 0.4	< 0.4
Transport accident	1.0012	1.0952
Disposal canister in final disposal	0.9959	1.0888

It can be seen that k_{eff} is highest in the transport accident situation. Since the disposal canister transport cask is under development and it is not clear that the analyzed transport accident needs to be considered, this situation is not further analyzed in this report.

Instead the final disposal location is used as the design case.

6.5 Position of fuel assemblies in the disposal canister

The fuel assembles are located in compartments in the disposal canister insert. There is a gap between the compartment wall and the fuel assembly so the fuel assembly location in the compartment could vary. The fuel assemblies located in the centre of the storage compartments is an ideal situation.

BWR
Different locations of the fuel assemblies in the compartments were investigated see figure 7. The assemblies are shifted 9.9 mm ((160-140.2)/2) in x and y directions towards the centre respectively away from the centre.

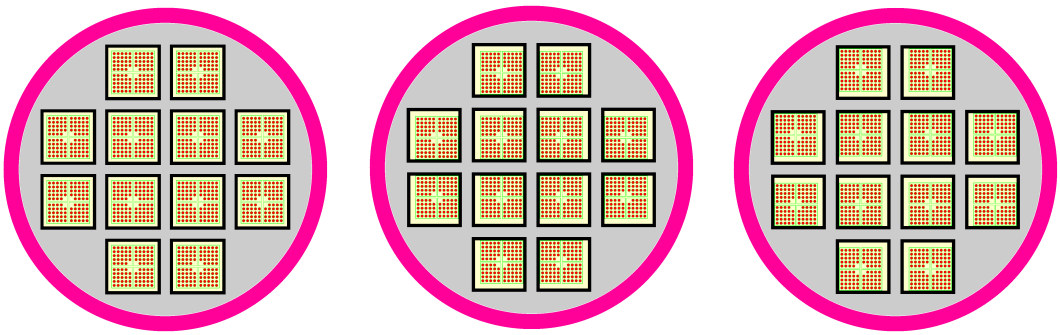

Figure 7 – Assembly locations, centre, in and out.

The resulting k_{eff} are shown in table 12.

Table 12 – k_{eff} at different assembly locations (σ=0.0002)

Location	k_{eff}
Centre	0.9969
In	1.0069
Out	0.9440

From reactivity standpoint the worst case is when the assemblies are located towards the centre of the disposal canister.

PWR
Different locations of the fuel assemblies in the compartments were investigated see figure 8. The assemblies are shifted 10.25 mm ((235-15x14.3)/2) in x and y directions towards the centre respectively away from the centre.

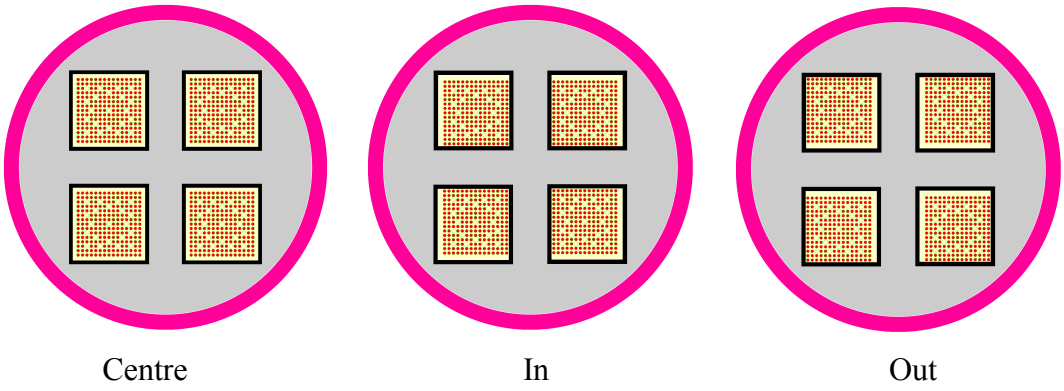

Figure 8 – Assembly locations, centre, in and out.

The resulting k_{eff} are shown in table 13.

Table 13 – k_{eff} at different assembly locations (σ=0.0005)

Location	k_{eff}
Centre	1.0888
In	1.0985
Out	1.0573

From reactivity standpoint the worst case is when the assemblies are located towards the centre of the disposal canister.

6.6 Disposal canister manufacturing tolerances

The manufacturing tolerances of the disposal canister are shown in table 1. The purpose with this section was to check the influence of the tolerances on the reactivity in order to find the combinations of measurements within the tolerance limits that will give the highest k_{eff}.

6.6.1 Centre to centre distance between compartments

The centre to centre distance between the compartments was varied. The results are presented in table 14. The wall thickness between compartments for each c-c distance is also shown in the table.

Table 14 – k_{eff} at different c-c distance between compartments (σ=0.0005)

c-c distance (mm)	Wall thickness between compartments including the Compartment tube wall (mm)	k_{eff}
PWR		
366.4	131.4	1.0904
370	135	1.0888
373.6	138.6	1.0871
BWR		k_{eff}
206	26	1.0014
210	30	0.9969
211	31	0.9942

The trend indicates that the minimum distance between the compartments will give the maximum k_{eff}.

6.6.2 Compartment size

The compartment size was varied. The results are presented in table 15.

Table 15 – k_{eff} at different compartment sizes (σ=0.0002)

PWR	k_{eff}
229.9	1.0932
235	1.0888
240.1	1.0829
BWR	
156.2	1.0031
160	0.9959
163.8	0.9874

It can be seen that the minimum compartment size gives the highest k_{eff}.

6.6.3 Compartment tube wall thickness

The compartment tube wall thickness was varied, with nominal c-c distance between compartments. The results are presented in table 16.

Table 16 – k_{eff} at different tube wall thickness (σ=0.0002)

PWR	k_{eff}
11.25	1.0887
12.5	1.0888
13.75	1.0889
BWR	k_{eff}
9	0.9961
10	0.9959
11	0.9949

The variations in k_{eff} are small compared to the statistical spread (σ=0.0002) of the result except for BWR where an increased wall thickness gives a decrease in k_{eff}.

6.6.4 Insert diameter

The insert diameter was varied. The results are presented in table 17.

Table 17-k_{eff} at different insert diameters (σ=0.0002)

Insert diameter (mm)	k_{eff}	
	PWR	BWR
949	1.0888	0.9959
949.5	1.0889	0.9961

The variations in k_{eff} are small compared to the statistical spread (σ=0.0002) of the result. This means that the variation insert diameter does not give a significant change in k_{eff}. The variations that can be seen in k_{eff} in the table are caused by the statistical variations in the calculation method in the code. The increase of the insert diameter gives insignificant changes to k_{eff}.

6.6.5 Copper shell thickness

The disposal canister geometry in this case was:

Table 18-k_{eff} at different copper thickness (σ=0.0002)

Copper thickness (mm)	k_{eff}	
	PWR	BWR
48.7	1.0887	0.9964
49	1.0888	0.9968
49.3	1.0889	0.9972

It can be seen that changes in copper shell thickness within the tolerance limits give insignificant variations in k_{eff}.

6.6.6 Compartment length

Table 19 – k_{eff} at different compartment lengths (σ=0.0002)

PWR	
Compartment length (mm)	k_{eff}
4433	1.0886
4443	1.0888
4448	1.0885
BWR	
Compartment length (mm)	k_{eff}
4453	0.9960
4463	0.9959
4468	0.9952

It can be seen that changes in compartment length within the tolerance limits give insignificant variations in k_{eff}.

6.6.7 Disposal canister length

Table 20 – k_{eff} at different disposal canister lengths (σ=0.0002)

Disposal canister length (mm)	k_{eff}	
	PWR	BWR
4832.25	1.0886	0.9951
4835	1.0888	0.9959
4838.25	1.0889	0.9949

It can be seen that changes in disposal canister length within the tolerance limits give small variations in k_{eff}.

6.7 Dependence on temperature

The compartment temperature was varied. The results are presented in figure 9.

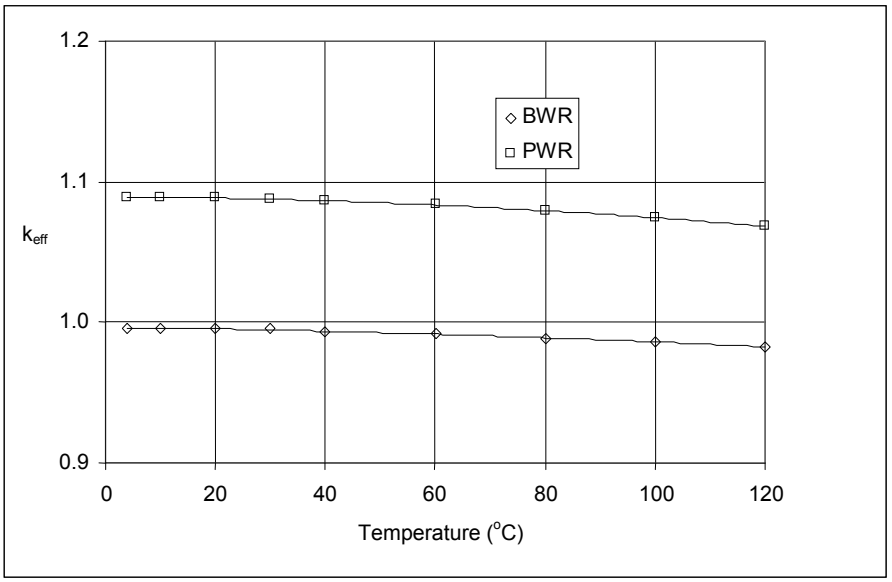

Figure 9 – k_{eff} vs. temperature in a disposal canister.

It can be seen that the reactivity decreases with increased temperature.

Max k_{eff} is achieved at 4 °C or 277 K.

6.8 Design case

Based on the above analysis the disposal canister design case was established:

The most reactive fuel assembly is used: F15x15AFA3G for PWR and Svea-96 Optima 3 for BWR

The fuel assemblies are radial located towards the centre of the disposal canister.

Assemblies are axially located at the centre of the disposal canister

The disposal canister is filled with water.

The temperature is 277 K.

The disposal canister is surrounded by 35 cm bentonite.

The boundary condition is vacuum.

The disposal canister data on the tolerance side that gives maximum reactivity:

Minimum c-c distance between compartments (364 mm for PWR and 206 mm for BWR)
Minimum compartment size (229.9 mm for PWR and 156.2 mm for BWR)
Nominal insert diameter (949 mm)
Minimum Fe content in the nodular cast iron (90%)
Nominal compartment tube wall thickness (12.5 mm for PWR and 10.0 mm for BWR)
Nominal copper shell inner diameter (952 mm)
Gap between insert and copper shell modeled as water
Nominal copper shell thickness (49 mm)
Nominal compartment length (4443 mm for PWR and 4463 mm for BWR)
Nominal insert length (4573 mm)
Nominal length of copper disposal canister (4835 mm)

The k_{eff} for the design case for 5% enriched fresh fuel is

PWR: $k_{eff} \pm \sigma = 1.1041 \pm 0.0002$
BWR: $k_{eff} \pm \sigma = 1.0232 \pm 0.0002$

This design case was used to determine the loading curves.

6.9 Variation with enrichment

In order to assess the dependence of k_{eff} on the initial enrichment k_{eff} was calculated varying the enrichment. The design model was used. The results are shown in figure 10. This information is used when the loading curve is developed in section 10.

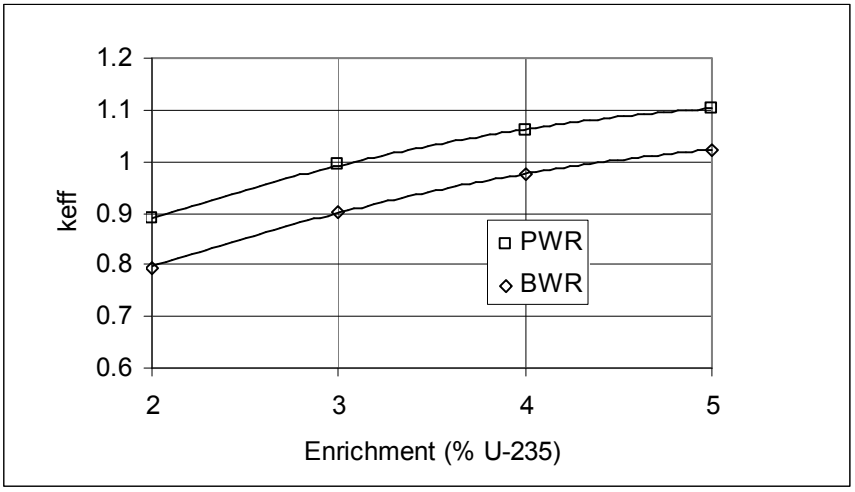

Figure 10 – k_{eff} as function of initial enrichment.

From figure 10 it can be estimated that k_{eff}= 0.94 (0.95 with allowance for calculation uncertainties) is achieved at the enrichment 2.4% for PWR and 3.5% for BWR. This corresponds to the highest enrichment that can be stored without burnup credit.

6.10 Variation of the number of fuel assemblies

To assess the effect of partly loaded disposal canisters calculations were performed with 3, 2 and 1 fuel assemblies the disposal canister. The design model was used and the empty locations were filled with water of 20 °C (293 K).

The purpose with these calculations is to find ways to create margins to handle fuel that not meet the burnup requirements in the loading curve.

The results are shown in table 21.

Table 21– k_{eff} for partly loaded BWR-disposal canister (σ=0.0002)

Case	No of fuel assemblies	k_{eff}
1	12	1.0232
2	11	0.9709
3	10	0.8941

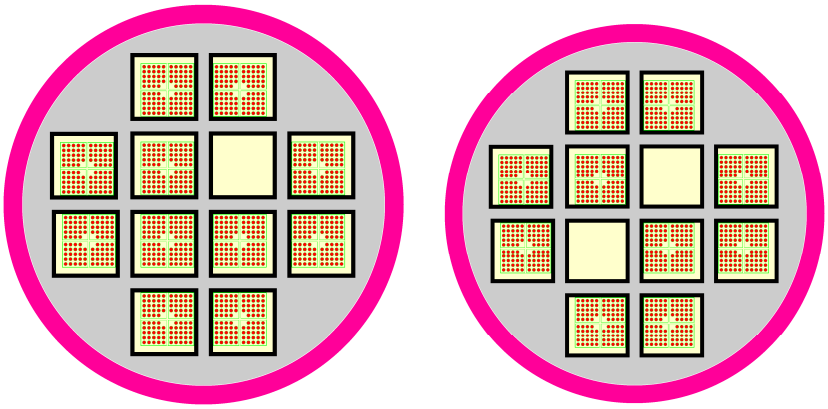

Figure 11 – Empty positions in case 2 and 3.

From these results it can be concluded that unirradiated BWR-fuel with 5% U-235 enrichment can be stored in a BWR-disposal canister with two central positions left empty.

Table 22 – k_{eff} for partly loaded PWR-disposal canister (σ=0.0004)

Case	No of fuel assemblies	k_{eff}
1	4	1.1041
2	3	1.0713
3	2 side by side	1.0474
4	2 diagonal	1.0091
5	1	1.0026

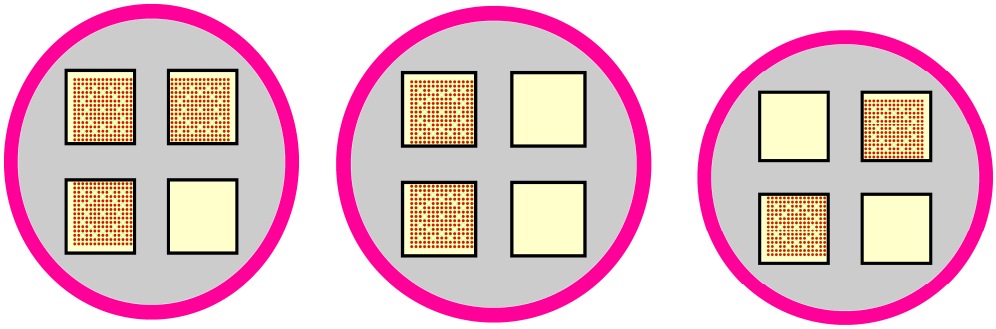

Figure 12 – Empty positions in case 2, 3 and 4.

From these results it can be seen that for PWR one unirradiated fuel assembly in a disposal canister with 5% U-235 enrichment will result in k_{eff} >0.95. The dependence of the enrichment for a disposal canister loaded with one fuel assembly was investigated. The results are shown in figure 13.

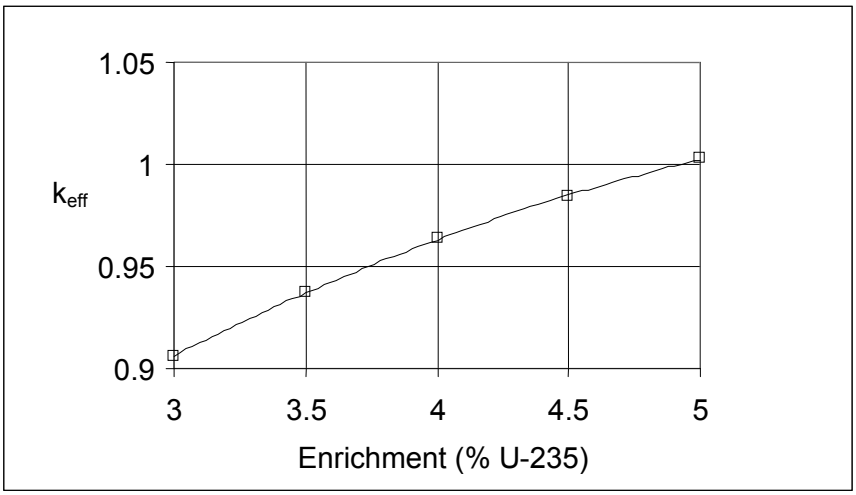

Figure 13 – k_{eff} as function of enrichment for a disposal canister with one PWR fuel assembly.

The results indicate that one fresh PWR fuel assembly with enrichment up to around 3.5% U-235, depending on the uncertainties will result in $k_{eff} < 0.95$ in a disposal canister.

7 Burnup Credit - Selection of nuclides

In previous reports /1/ and /2/ and in the sections above it was shown that “fresh fuel”-assumption could not be used in the disposal canister for final repository. Credit for the reactivity decrease due to the burnup of the fuel is necessary to meet the criticality criteria. In this section it is investigated if the burnup of the fuel will give enough decrease of the reactivity to meet the reactivity criteria.

In the irradiation process around 1300 isotopes are created in the irradiated fuel.
All isotopes cannot be represented in the models and it is needed to establish a limited set to use in burnup credit. To select which isotopes to credit the following requirements could be established as criteria:

1. The isotopes should contribute to the reactivity decrease

   The importance of different isotopes has been assessed in several studies. The reactivity worth of different isotopes varies with fuel design, initial enrichment, operational history and cooling time. The important nuclides seem, however to remain the same.

2. Knowledge of nuclear data of the isotopes

   Nuclear data such as neutron cross sections and half-life have to be well known in order to be able to predict the isotopic contents in the fuel.

3. Knowledge of their chemical form, physical form and characteristics, solubility and volatility

   Subcriticality in the final repository needs to be verified for very long time periods. During this time it has to be certain that the isotopes are stable in the fuel.

4. The calculated isotopic content in the irradiated fuel should be verified

   The calculation of isotopic composition in irradiated nuclear fuel should be verified by comparison with experimental data if the nuclides are used in burnup credit. This provides a robust basis for disposal canister design and disposal.

If these criteria are accepted, the following nuclides could presently be used for burnup credit in final disposal canisters. The basis for the selection is found in /6/.

Set 1: Actinides

U-234, U-235, U-236, U-238, Pu-238, Pu-239, Pu-240, Pu-241, Pu-242, Am-241, Np-237

Criticality calculations are performed with credit only for the above limited number of isotopes to assess if burnup credit is sufficient to control reactivity. If not selected fission products could also be credited.

Set 2: Actinides + fission products

U-234, U-235, U-236, U-238, Pu-238, Pu-239, Pu-240, Pu-241, Pu-242, Am-241, Np-237
Mo-95, Tc-99, Ru-101, Rh-103, Ag-109, Cs-133, Nd-143, Nd-145, Sm-147, Sm-149,
Sm-150, Sm-151, Eu-151, Sm-152, Eu-153, Gd-155

8 Calculations of k_{eff} vs burnup

Burnup dependent cross sections were created for F15*15AFA3G for different enrichments and irradiation histories using SAS2. The irradiation was simulated in reactor conditions. Specific power, cycle history and reactor condition from table 7 were used.

The moderator density was set to correspond to the core exit temperature. The temperatures of fuel and materials during irradiation are based on typical plant data.

The enrichments 3.0%, 4.0%, and 5.0% U-235 were analyzed for PWR and 4.0%, 4.5%, and 5.0% for BWR.

The decay time was one year after the last cycle.

In Starbucs burnup calculations are made for each zone in a fuel assembly. Based on the cross sections generated with SAS2, problem specific cross sections are generated as input to a 3D Keno V.a-model and k_{eff} could be calculated for a specific disposal canister model.

In this case the design case model of a PWR disposal canister, according to section 6.8 was used.

The resulting k_{eff} function of burnup is shown figure 14 for actinides (set 1).

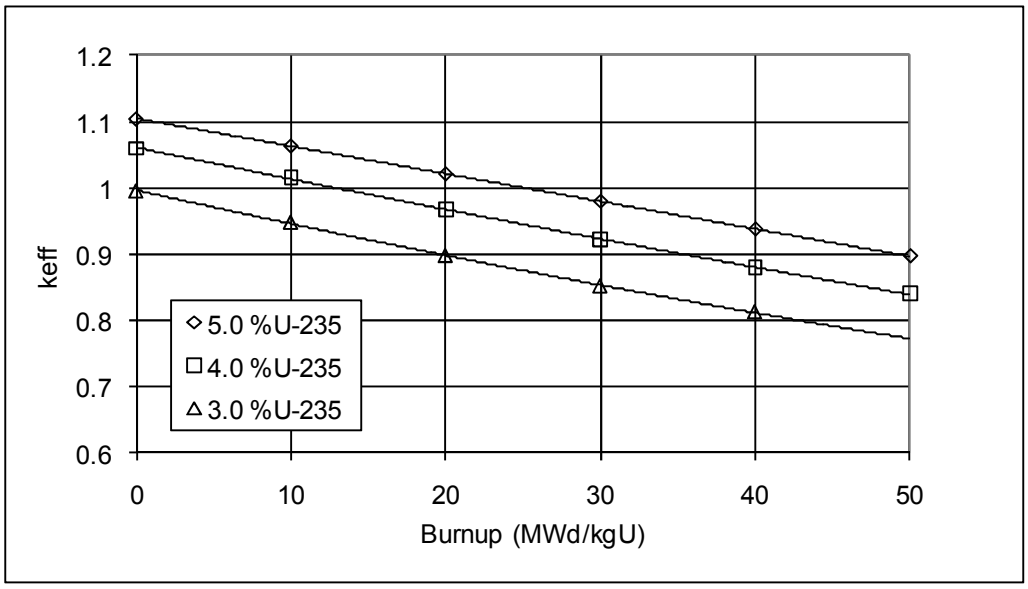

Figure 14 – k_{eff} as function of burnup, PWR, actinides only (set 1).

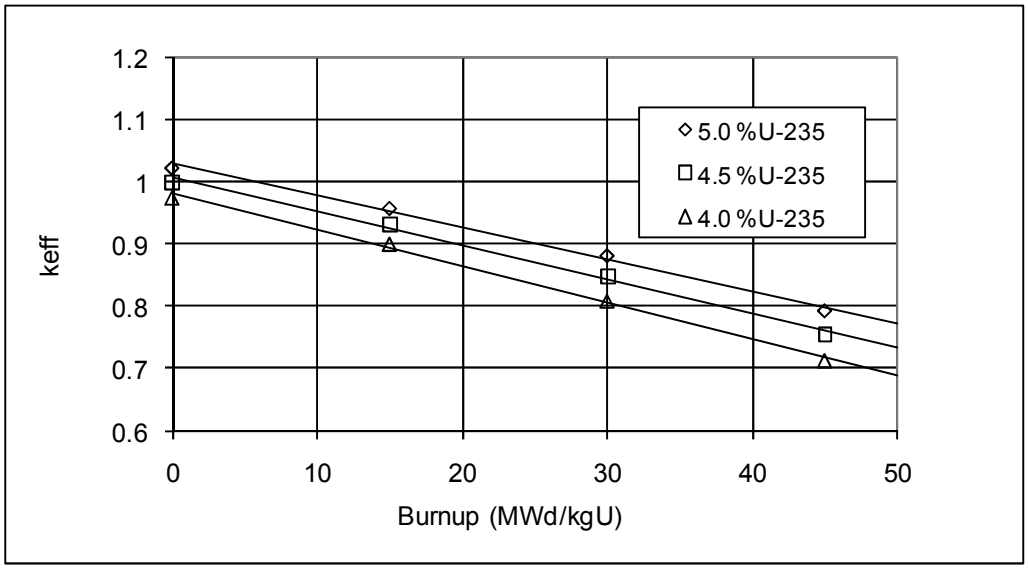

Figure 15 – k_{eff} as function of burnup, BWR actinides only (set 1).

The k_{eff} shows a almost linear behavior with the burnup. Fit of straight lines to the calculated points give the following slopes shown in table 23 and 24.

Table 23 – Slopes of the burnup curve for PWR (set 1)

Enrichment (%U-235)	Slope (dk/MWd/kg)
3.0	-0.0046
4.0	-0.0044
5.0	-0.0042

Table 24 – Slopes of the burnup curve for BWR (set 1)

Enrichment (%U-235)	Slope (dk/MWd/kg)
3.0	-0.0059
4.0	-0.0055
5.0	-0.0051

Diagram for actinides and fission products (set 2) is shown below in figure 16.

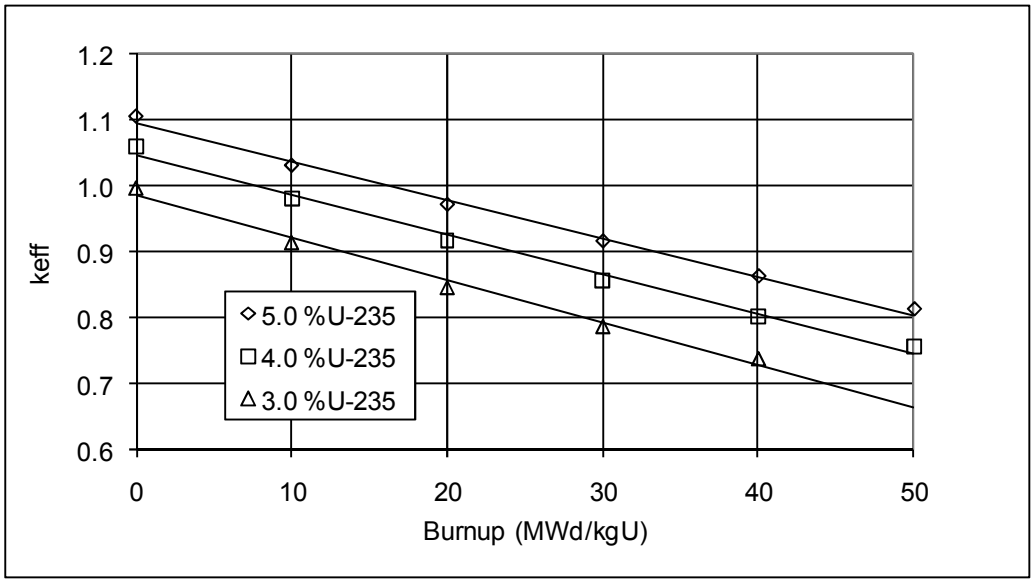

Figure 16 – k_{eff} as function of burnup, actinides and fission products PWR (set 2).

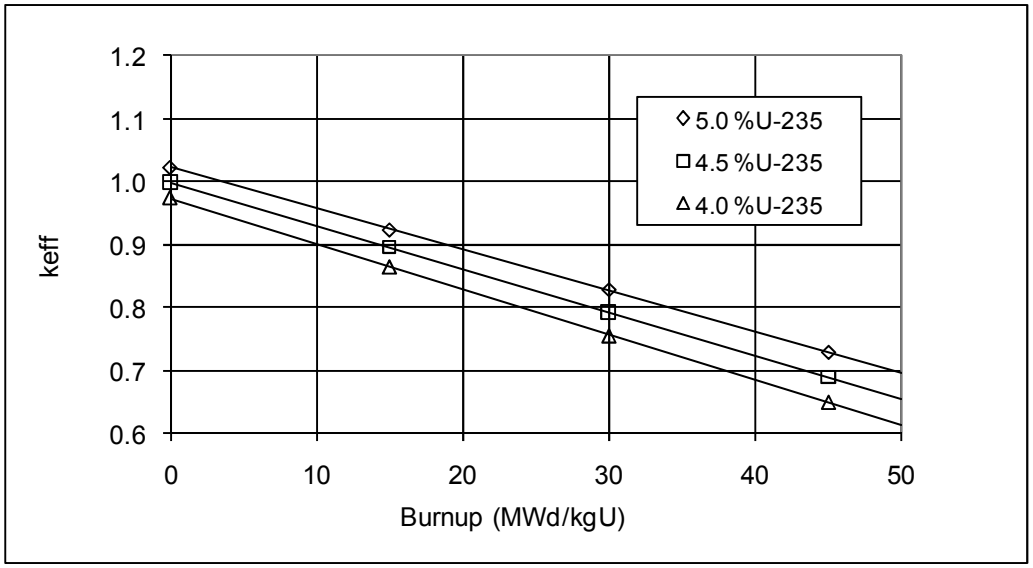

Figure 17 – k_{eff} as function of burnup, actinides and fission products BWR (set 2).

Fits of straight lines to the calculated points give the following slopes shown in table 25 and 26.

Table 25 – Slopes of the burnup curve for PWR (set 2)

Enrichment (%U-235)	Slope (dk/MWd/kg)
3.0	-0.0064
4.0	-0.0060
5.0	-0.0058

Table 26 – Slopes of the burnup curve for BWR (set 2)

Enrichment (%U-235)	Slope (dk/MWd/kg)
4.0	-0.0073
4.5	-0.0068
5.0	-0.0065

9 Uncertainties

9.1 Disposal canister

The results above are based on the most reactive location of the disposal canisters during handling and the most reactive location of the fuel assemblies in the disposal canister. The disposal canister geometry is modeled with measures on the tolerance side that gives the highest reactivity. No correction factor for tolerances in the disposal canister measures is needed.

9.2 Specific power

The effect of different specific powers (power densities) during irradiation was investigated in /7/. The results show that the predicted k-value increases if lower specific power is used. In this study a relatively low power density of 14 MW/assembly was used for PWR compared to the Ringhals 2 value which in average is 17 MW/assembly and Ringhals 3/4 18 MW/assembly which will be increased to 20 MW/assembly. For BWR 3.8 MW/assembly was used compared to the Oskarhamn reactors which have 3.2 MW/assembly for Oskarhamn 1 and 4.8 MW/assembly for Oskarshamn 3 which will be increased to 5.6 MW/assembly

9.3 Integral burnable poison

BWR- and some PWR-fuel assemblies contain integral burnable poison. In /8/ it is shown that multiplication factor for fuel containing Gd_2O_3 is always lower than the multiplication factor for fuel without Gd_2O_3 throughout burnup. Burnable poison was not modeled in this study why no additional uncertainty is needed.

9.4 Burnable poison rods

In initial PWR-cores in Ringhals burnable poison rods were used in about 60 of the 157 fuel assemblies. The poison rods are made of stainless steel, borosilicate glass and zircaloy. In /9/ it is shown that the presence of burnable poison rods give higher multiplication factor compared with fuel without poison rods throughout burnup. The burnable poison is depleted during the first cycle. If the burnable rod cluster not is removed after the first cycle a significant portion of the reactivity difference is shown to be due to the displacement of moderator. The reactivity difference is shown to be up to 3%Δk. This has to be considered when fuel assemblies that have contained burnable poison rods will be compared with the loading curve. No general uncertainty is therefore needed to cover this effect.

9.5 Declared burnup

The declared assembly average burnup is based on the plant heat balance, measurements and calculations of the power distribution in the core. Based on uncertainties of the measurements and calculations the uncertainty in the burnup prediction is estimated to be within σ_{BU}=2% for BWR and $2\sigma_{BU}$=3.65% for PWR. (Sources: OKG 2008-05-26, reg nr 2008-14670 and Ringhals 2007-10-19, 1960160/1.1. Confidential information. Available only for the Swedish Radiation Safety Authority.)

With the diagrams in figures 14-17 the reactivity value of the uncertainties in burnup was calculated. The results are shown in table 27.

Table 27 – Uncertainty in burnup ($2\sigma_{BU}$) for BWR

Burnup (MWd/kgU)	BWR						
	Uncertainty	Actinides			Actinides and fissionproducts		
	(MWd/kgU)	5% U-235	4.5% U-235	3% U-235	5% U-235	4.5% U-235	3% U-235
10	0.4	0.0020	0.0022	0.0023	0.0026	0.0028	0.0029
20	0.8	0.0041	0.0044	0.0047	0.0053	0.0055	0.0058
30	1.2	0.0061	0.0065	0.0070	0.0079	0.0083	0.0087
40	1.6	0.0082	0.0087	0.0094	0.0105	0.0110	0.0116
50	2	0.0102	0.0109	0.0117	0.0131	0.0138	0.0144

Table 28 – Uncertainty in burnup ($2\sigma_{BU}$) for BWR

Burnup	PWR						
(MWd/kgU)	Uncertainty	Actinides			Actinides and fissionproducts		
	(MWd/kgU)	5% U-235	4% U-235	3% U-235	5% U-235	4% U-235	3% U-235
10	0.4	0.0015	0.0016	0.0017	0.0021	0.0022	0.0023
20	0.7	0.0030	0.0032	0.0034	0.0042	0.0044	0.0047
30	1.1	0.0046	0.0049	0.0051	0.0063	0.0066	0.0070
40	1.5	0.0061	0.0065	0.0067	0.0084	0.0088	0.0094
50	1.8	0.0076	0.0081	0.0084	0.0105	0.0110	0.0117

9.6 Axial temperature distribution in fuel assemblies

Due to the higher temperature and lower moderator density in the top of the core more Pu-239 will be produced than in average. This could lead to a non conservatism if the calculations were done using average core temperature.

In this study for PWR the core exit temperature and the corresponding water density was used. The axial distribution of isotopes will thus not require any additional uncertainty.

For BWR the axial void distribution and not the temperature distribution is important for the Pu-239 production.

9.7 Axial void distribution in BWR-assemblies

In this study the core exit void content and the corresponding water density was used. The axial distribution of isotopes will thus not require any additional uncertainty.

9.8 Axial burnup distribution (end effect)

The burnup for each assembly is normally given as an assembly average value. This value and the initial enrichment are used to verify the reactivity of the fuel assembly.

It is shown in several reports (e.g. /10/) that ”end effect” can occur because of the axial burnup distribution in the reactors which is a consequence of the axial power distribution in the reactor. This leads to a situation there the end zones in the fuel get lower burnup due to the axial neutron leakage and

lower local power. If this is considered the reactivity of the assembly could be larger than compared to the case when the assembly has a uniform burnup distribution.

The consequence is that the given average burnup might not be a good parameter to assess the assembly reactivity. The axial burnup distribution has to be considered. The end effect can be defined as:

$$\Delta k_{\text{end effect}} = k_{\text{eff}}^{(\text{with axial burnup distribution})} - k_{\text{eff}}^{(\text{uniform axial burnup})}$$

PWR

To determine the end effect in the disposal canister for PWR fuel axial burnup distributions from 15 cores from Ringhals 2, 3 and 4 were studied. In addition 9 cores from the Great- and Frej-projects were studied, see appendix 4. The fuel types are 15x15 and 17x17-fuel with burnup from 10 MWd/kgU up to 65 MWd/kgU. Initial enrichments are 3.2 – 4.95% U-235.

From this population a number of distributions were chosen for analysis. Distributions with the highest and lowest peaking factors (F), with the lowest burnup in the bottom node, with the lowest burnup in the top node were selected, this because the end effect is highly dependent on the burnup in the top and the bottom nodes. A bounding burnup distribution was constructed by reducing the burnup in the bottom and top node by 20% while keeping the assembly burnup constant. The resulting distributions are shown in figure 18.

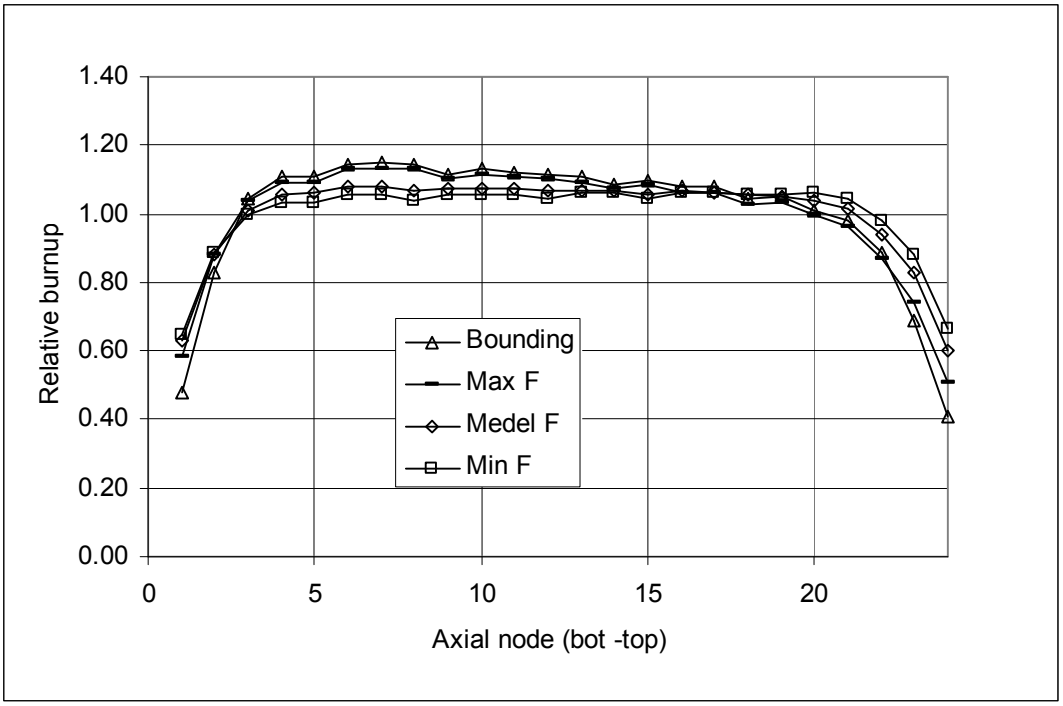

Figure 18 – PWR axial burnup distributions.

These axial burnup distributions were used in the fuel in the disposal canister model. The design case model of the disposal canister, according to section 6.8 was used.

The k_{eff} was calculated for each distribution at burnup from 10 to 50 MWd/kgU.

The calculated k_{eff} was compared to the k_{eff} for a uniform burnup distribution at each burnup step. The difference in k_{eff} between the k_{eff} with axial distribution and the k_{eff} with uniform distribution (end effect) is shown in figure 19 for actinides.

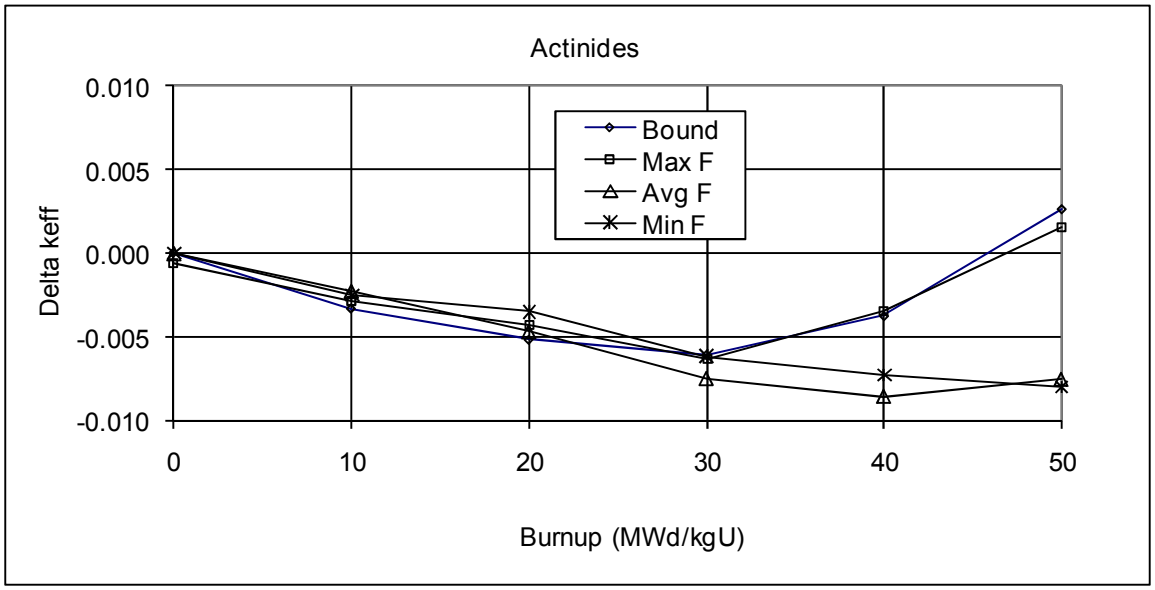

Figure 19 – The end effect as function of burnup for different axial burnup distributions for PWR (actinides, set 1).

It can be seen that the end effect is negative up to 45 MWd/kgU. At burnup above this value a correction of the k_{eff} due to the end effect is required.

For actinides and fission products (set 2) the results for the bounding axial burnup distribution is shown in figure 20.

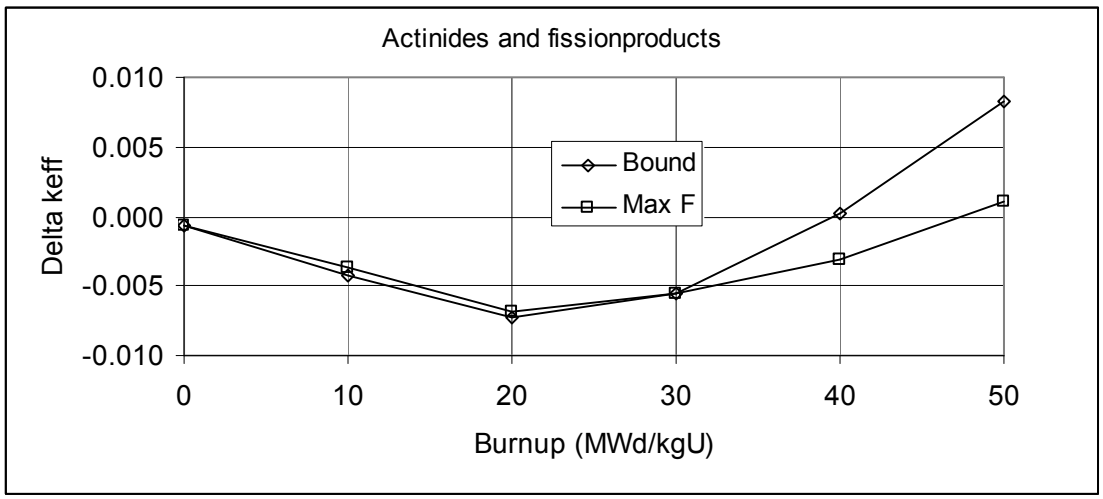

Figure 20 – The end effect as function of burnup for different axial burnup distribution for PWR, (actinides and fission products, set 2).

It can be seen that the end effect is negative up to 40 MWd/kgU. At burnup above this value a correction of the k_{eff} due to the end effect is required.

The dependence between the end effect and the decay time of the fuel is evaluated in section 9.15.

BWR

To determine the end effect in the disposal canister for BWR fuel axial burnup distributions from 18 cores from Oskarshamn 2 and 3, Ringhals 1 and Forsmark 1, 2 and 3 were studied, see appendix 4.

From this population a number of distributions were chosen for analysis. Distributions with the highest and lowest peaking factors (F), with the lowest burnup in the bottom node, with the lowest burnup in the top node were selected, this because the end effect is highly dependent on the burnup in the top and the bottom nodes. The resulting distributions are shown in figure 21.

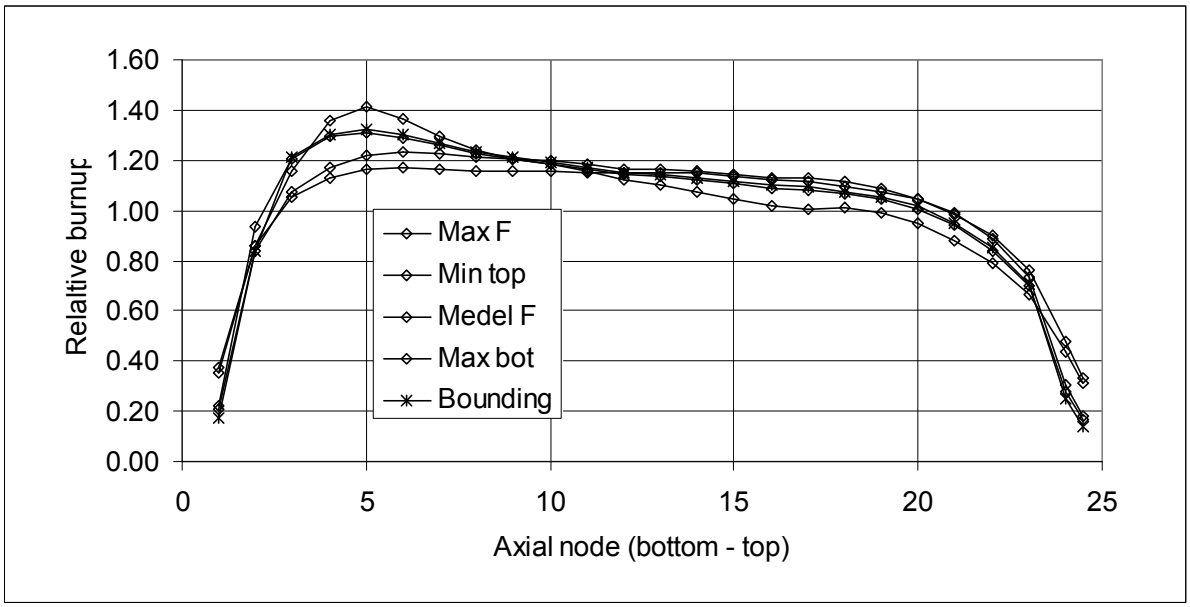

Figure 21– BWR axial burnup distributions.

These axial burnup distributions were used for the fuel assemblies in the disposal canister model. The design case model of the disposal canister, according to section 6.8 was used.

The k_{eff} was calculated for each distribution at burnup from 10 to 50 MWd/kgU.

The calculated k_{eff} was compared to the k_{eff} for a uniform burnup distribution at each burnup step. The difference in k_{eff} between the k_{eff} with axial distribution and the k_{eff} with uniform distribution (end effect) is shown in figure 22 for actinides.

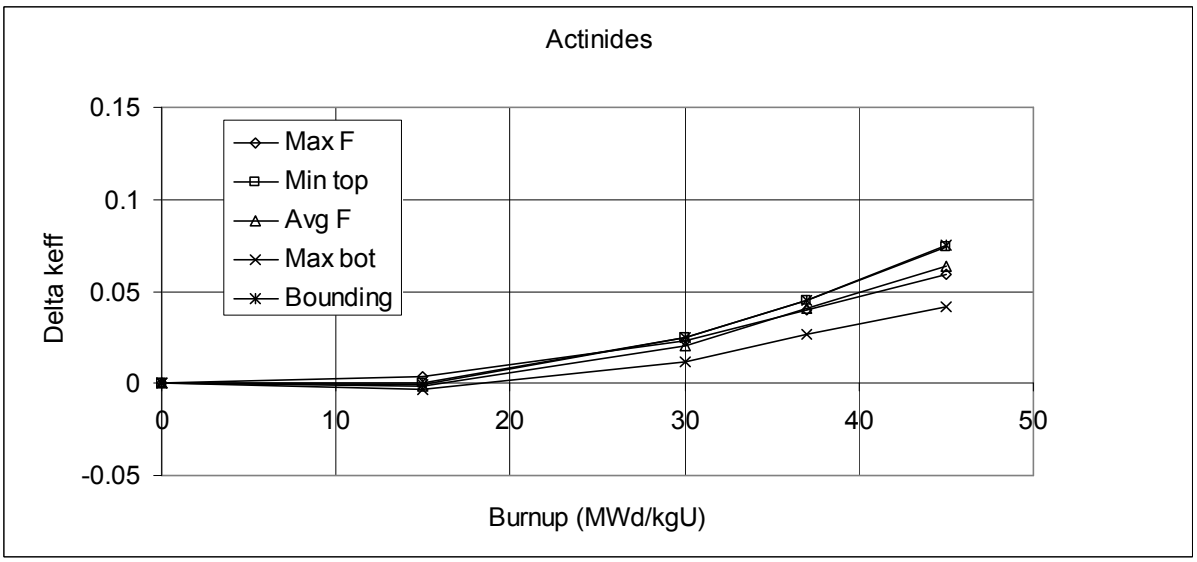

Figure 22 – The end effect as function of burnup for different axial burnup distributions for BWR (actinides, set 1).

It can be seen that the end effect has a positive value and a correction of the k_{eff} due to the end effect is required.

For actinides and fission products (set 2) the results for the bounding axial burnup distribution is shown in figure 23.

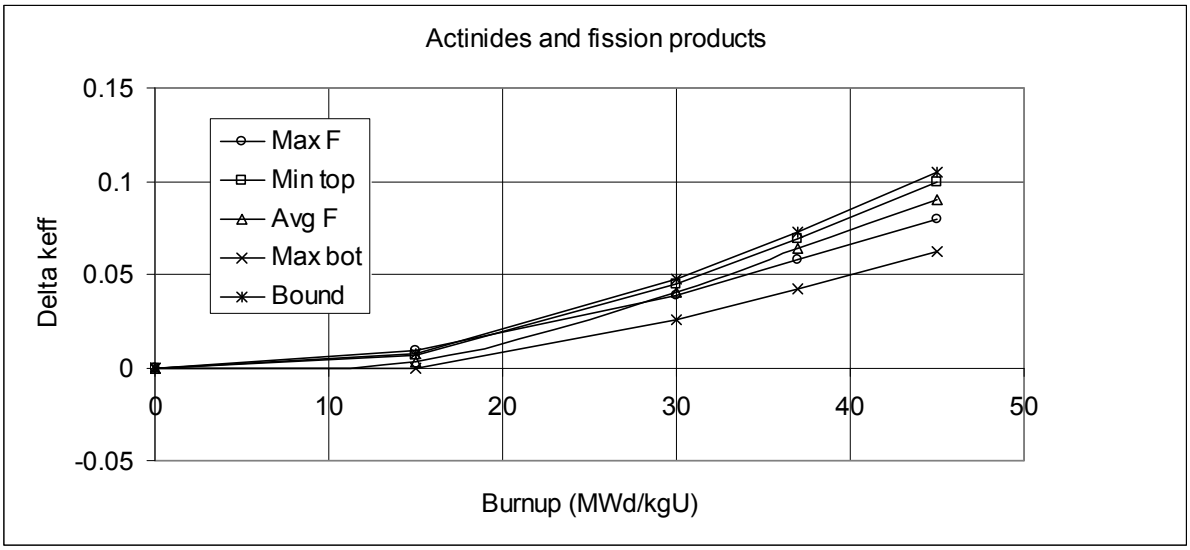

Figure 23 – The end effect as function of burnup for different axial burnup distribution for BWR, (actinides and fission products, set 2).

It can be seen that the end effect has a positive value and a correction of the k_{eff} due to the end effect is required.

BWR-assemblies normally have lower enrichments in the end zones, which will reduce the end effect. This is not credited in this analysis.

The dependence between the end effect and the decay time of the fuel is evaluated in section 9.15.

9.9 Control rods

Normally during operation control rods in both BWR and PWR are not inserted in the core. The effect of inserted control rods has therefore not been evaluated.

9.10 Horizontal burnup distribution

In this case the design case model of a disposal canister, according to section 6.8 was used.

In the assembly a horizontal gradient of the burnup could be generated if the assembly is located in an area with a power gradient. This means that one side of the assembly could have lower burnup than the average which in some cases could give a reactivity increase in the disposal canister. It is assumed that the burnup could vary 10% from the average at one side of the assembly with the same average value. The assemblies are located with the lowest burnup towards the centre of the disposal canister, see figure 24. This configuration gives the highest k-value.

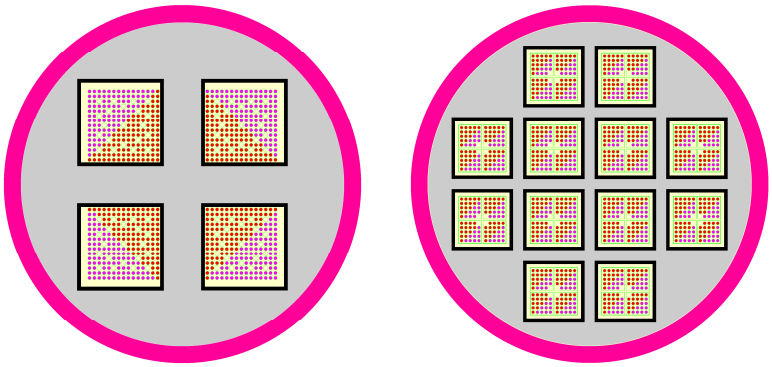

Figure 24 – Locations of fuel assemblies in the disposal canister.

Calculations of k_{eff} in this configuration were done for different burnup. The results are shown in tables 29 and 30, where the difference in k_{eff} between the cases with a horizontal burnup distribution and the case with a uniform horizontal burnup distribution are shown.

Table 29 – Effect of radial burnup gradient for BWR

Burnup	Actinides			Actinides and fissionproducts		
MWd/kgU	Nominal k_{eff}	Gradient k_{eff}	Difference Δk_{eff}	Nominal k_{eff}	Gradient k_{eff}	Difference Δk_{eff}
15	0.9580	0.9596	0.0016	0.9231	0.9253	0.0021
30	0.8816	0.8834	0.0018	0.8272	0.8309	0.0036
45	0.7926	0.7974	0.0048	0.7268	0.7316	0.0048

Table 30 – Effect of radial burnup gradient for PWR

Burnup	Actinides			Actinides and fissionproducts		
MWd/kgU	Nominal k_{eff}	Gradient k_{eff}	Difference Δk_{eff}	Nominal k_{eff}	Gradient k_{eff}	Difference Δk_{eff}
10	1.0633	1.0643	0.0010	1.0298	1.0300	0.0003
20	1.0210	1.0222	0.0012	0.9705	0.9728	0.0022
30	0.9794	0.9814	0.0020	0.9151	0.9179	0.0028
40	0.9375	0.9403	0.0028	0.8618	0.8660	0.0041
50	0.8968	0.9013	0.0045	0.8119	0.8170	0.0051

Horizontal burnup distributions increase k_{eff}. This needs to be considered as an uncertainty factor when developing the loading curve.

(It should be noted that the radial difference in the burnup from the average is ± 10% in the calculations which is higher than values reported in sources: Ringhals 2007-10-19, 1960160/1.1 and OKG 2008-05-26, reg nr 2008-14670. Confidential information. Available only for the Swedish Radiation Safety Authority.)

9.11 Demolition of fuel assemblies

Two cases of total demolitions of the fuel in the disposal canister were calculated. The design case model of a PWR- and BWR disposal canister, according to section 6.8 was used, except for the homogenized parts.

1. In each of the compartments the fuel assembly materials including the material in the compartment walls are mixed homogenously with the water in the compartment. Calculations were done for different amount of water in the compartments. The results are shown in figure 25 for PWR and BWR.

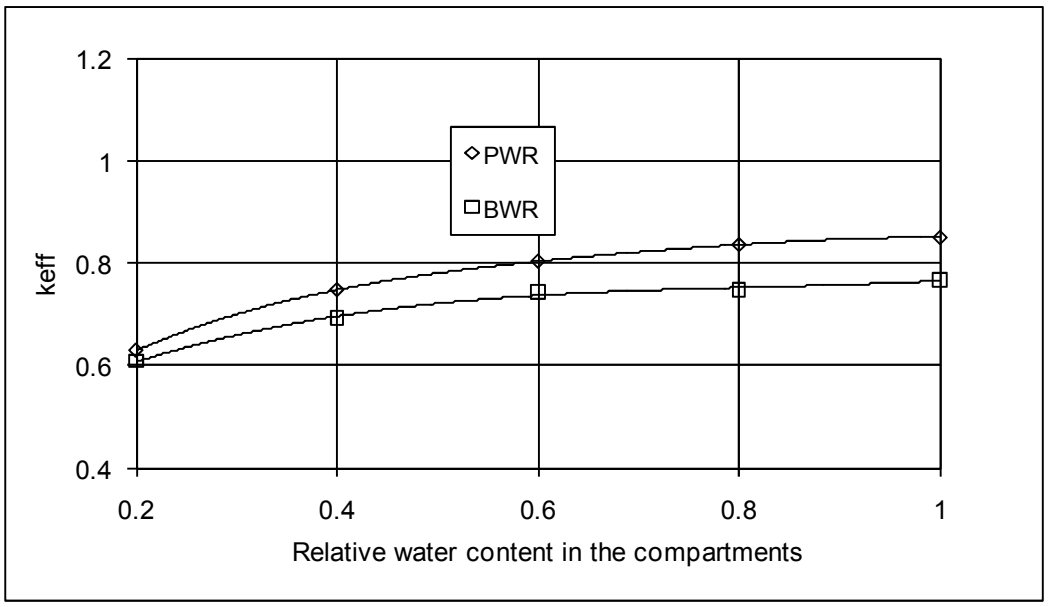

Figure 25 – k_{eff} in disposal canister with homogenous fuel/water mixture in the compartments.

It is shown that max k_{eff} is achieved when compartments are completely filled with water which is homogenously mixed with the fuel assembly and compartment wall materials. The max $k_{eff}\pm\sigma$= 0.8496± 0.0003 for PWR and $k_{eff}\pm\sigma$= 0.7660± 0.0003 for BWR which are less than the design cases for PWR and BWR respectively. No additional uncertainty is needed to cover this case.

2. All materials in the four fuel assemblies are homogenously mixed with the water in the compartments and the steel in the insert. In this case the resulting k_{eff} is <=0.5 for both PWR and BWR No additional uncertainty is needed to cover this case.

9.12 Calculation uncertainty

The average value and the standard deviation of the k_{eff} calculation in KENO are calculated from a number of neutron generations or iterations. In these cases the calculations were done with 3003 neutron generations. This is used to estimate the upper one sided tolerance limit. The constant K=1.72 is picked from /11/. The standard deviation is generally 0.0005Δk or less. The 95/95 upper one sided tolerance limit is then calculated 0.0005x1.703=0.0009Δk.

The average value of k_{eff} for 59 calculated experiments is 0.9993 which means a bias of -0.0007Δk. The standard deviation of the 59 cases is 0.0046Δk, see appendix 1. This value is used to estimate the lower one sided tolerance limit on 95%/95% -level. The constant K=2.026 is picked from /11/. Statistical uncertainty for the lower tolerance limit is then 0.0046x2.026= 0.0093Δk.

9.13 Manufacturing tolerances

9.13.1 Disposal Canister

The manufacturing tolerances of the disposal canister are discussed in section 9.1.

9.13.2 Fuel assembly

For the fuel assembly nominal values have been used. The effects of the tolerances have been evaluated in this section.

The tolerances for F15x15AFA3G and Svea 96 Optima 3 are given in table 31. (Source: SKBdoc 1173564, ver 1.0. Confidential information. Available only for the Swedish Radiation Safety Authority.)

Table 31 – Nominal values and tolerances

Parameter	Svea 64 Optima 3		F15x15AFA3G	
	Nominal value	Tolerance	Nominal value	Tolerance
Fuel rod diameter (mm)	9.84	±0.04	10.72	± 0.04
Pellet diameter (mm)	8.48	±0.013	9.294	± 0.012
UO_2 density (g/cm^3)	10.7	±0.1	10.7	± 0.11
Rod pitch (mm)	12.768	±0.04	14.3	± 0.04
Active fuel length (mm)	3690	±12.2	3658	± 7

The calculations in this section were done with the design model according to section 6.8, with 277 K in the disposal canister.

Calculations were done for the nominal value and for several values around the nominal value for all parameters in table 31. A least square fit of a straight line was done to get the slope of the line. The slope value was used to calculate the uncertainty in reactivity due to variations within the tolerances for respective parameter.

Fuel rod diameter

The effect on the reactivity due to change in the fuel rod outer diameter was calculated for BWR and PWR using the design models. The resulting k_{eff}-values are shown in figure 26.

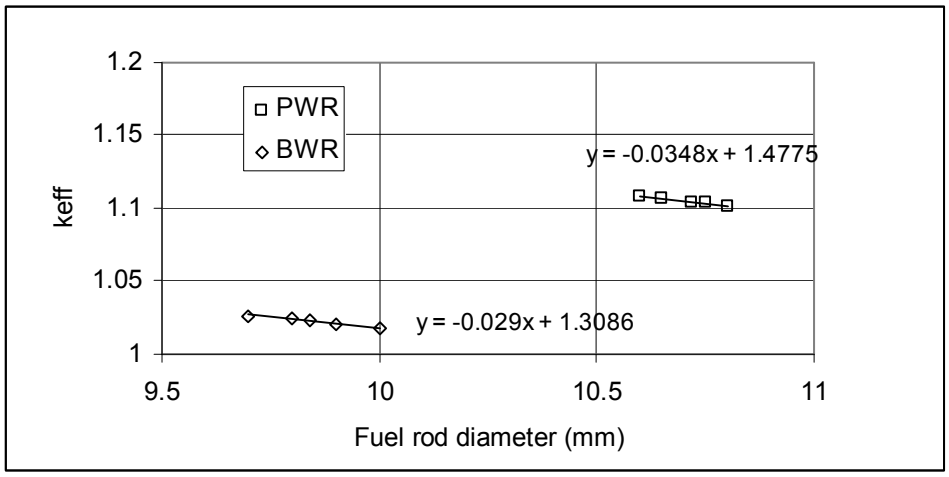

Figure 26 – k_{eff} as function of the fuel rod outer diameter.

Linear fits with straight lines to the calculated points give a slope of - 0.0348 Δk/mm for PWR and -0.029Δk/mm for BWR. A ±0.04 mm tolerance deviation gives en reactivity change of Δk ±0.0014 for PWR and Δk ±0.0012 for BWR.

Pellet diameter

The effect on the reactivity due to change in the pellet diameter was calculated for BWR and PWR using the design models. The resulting k_{eff}-values are shown in figure 27.

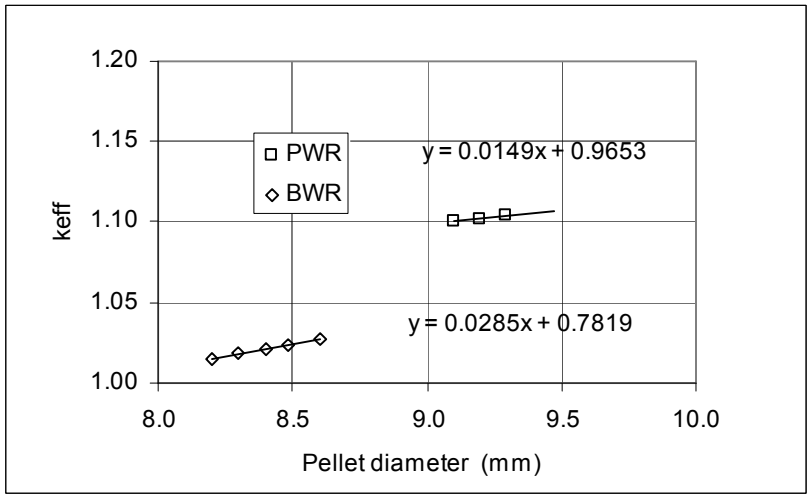

Figure 27 – k_{eff} as function of the fuel pellet diameter.

Linear fits with straight lines to the calculated points give a slope of - 0.0149 Δk/mm for PWR and -0.0285 Δk/mm for BWR. A ±0.012 mm tolerance deviation gives en reactivity change of Δk ±0.0002 for PWR and ±0.013 mm tolerance deviation gives en reactivity Δk ±0.0004 for BWR.

UO_2 density

The effect on the reactivity due to change in the UO_2 density diameter was calculated for BWR and PWR using the design models. The resulting k_{eff}-values are shown in figure 28.

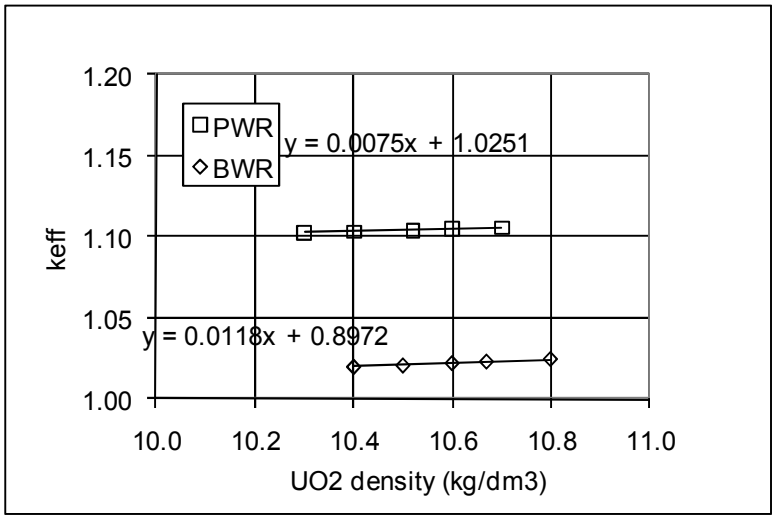

Figure 28 – k_{eff} as function of the UO_2 density.

Linear fits with straight lines to the calculated points give a slope of - 0.0075 Δk/mm for PWR and -0.0118 Δk/mm for BWR. A ±0.11 mm tolerance deviation gives en reactivity change of Δk ±0.0008 for PWR and ±0.1 mm tolerance deviation gives en reactivity Δk ±0.0012 for BWR.

Rod pitch

The effect on the reactivity due to change in fuel rod pitch was calculated for BWR and PWR using the design models. The resulting k_{eff}-values are shown in figure 29.

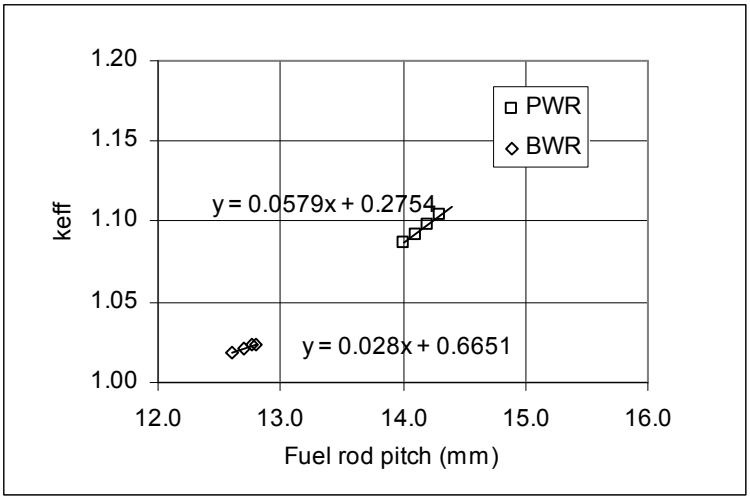

Figure 29 – k_{eff} as function of the fuel rod outer diameter.

Linear fits with straight lines to the calculated points give a slope of - 0.0579 Δk/mm for PWR and 0.028 Δk/mm for BWR. A ±0.04 mm tolerance deviation gives en reactivity change of Δk ±0.0023 for PWR Δk ±0.0011 for BWR.

Active fuel length

The effect on the reactivity due to change in the active fuel length was calculated for BWR and PWR using the design models. The resulting k_{eff}-values are shown in figure 30.

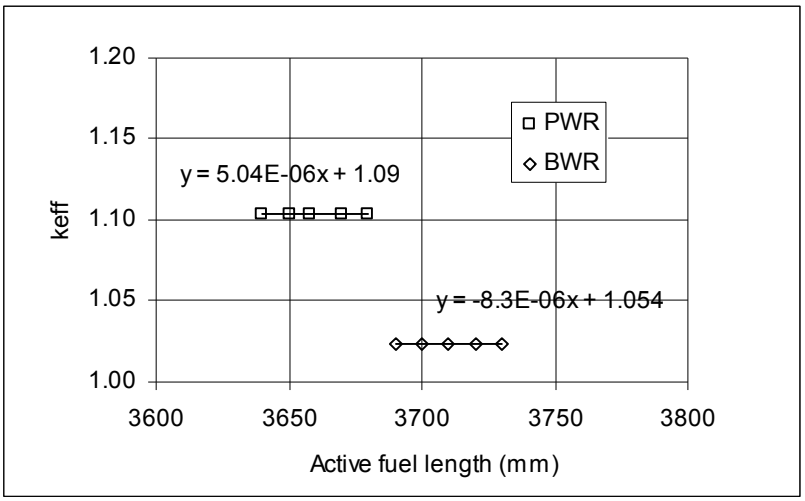

Figure 30 – k_{eff} as function of the fuel rod outer diameter.

Linear fits with straight lines to the calculated points give a slope of $5x10^{-6}$ Δk/mm for PWR and $-8x10^{-6}$ Δk/mm for BWR. A ±7 mm tolerance deviation gives en reactivity change of less than Δk ±0.0001 Δk for PWR and ±12.2 mm tolerance deviation gives en reactivity change Δk ±0.0001 for BWR.

The uncertainties are summarized in table 32.

Table 32 – Summary of the uncertainties

Parameter	Uncertainty	
	PWR	BWR
Fuel rod diameter	0.0014	0.0012
Pellet diameter	0.0002	0.0004
UO_2 density	0.0008	0.0012
Rod pitch	0.0023	0.0011
Active fuel length	0.0001	0.0001

The square root of sum of squares of these uncertainties is Δk_{eff} =0.0020 for BWR and 0.0028 för PWR.

9.14 Isotopic prediction

PWR
There are several sets of radiochemical analyses of irradiated fuel samples that could be used to verify the calculations. Measured data have been calculated with the sequence SAS2 /Origen –S reports in /12/, /13/ and /14/. Isotopes with no measured data are excluded in the analysis.

The comparisons are shown in table 33.

Table 33 – PWR comparison between measured and calculated nuclide contents /14/

Nuclide	No of samples	Measured/ calculated (average) X	Standard-deviation S(X)
Ag-109	N/A	N/A	
Am-241	28	0.919	0.204
Am-243	16	0.934	0.105
Cs-133	3	0.976	0.009
Eu-151	4	0.926	0.532
Eu-153	4	0.966	0.048
Gd-155	4	1.287	0.124
Mo-95	0	N/A[c]	N/A
Nd-143	14	1.012	0.013
Nd-145	14	0.996	0.009
Np-237	18	0.952	0.086
Pu-238	52	1.068	0.1
Pu-239 [f]	56	1.008	0.042
Pu-240	56	1.008	0.028
Pu-241 [f]	56	1.045	0.048
Pu-242	52	0.987	0.051
Rh-103	1	1.269	N/A
Ru-I01	0	N/A[c]	N/A
Sm-147	9	1.001	0.039
Sm-149	9	1.002	0.221
Sm-150	9	0.934	0.018
Sm-151	9	0.777	0.059
Sm-152	9	0.751	0.142
Tc-99	9	0.844	0.194
U-234	32	0.962	0.113
U-235 [f]	56	1.018	0.03
U-236	56	1.008	0.037
U-238	56	1	0.005

[f] fissile nuclides, [c] Insufficient data

To assess the effect of the results in table 33, the correction factors (X) for all nuclides were used when calculating the k_{eff}. In this case the design case model of a PWR-disposal canister, according to section 6.8 was used.

The results are shown in figure 31.

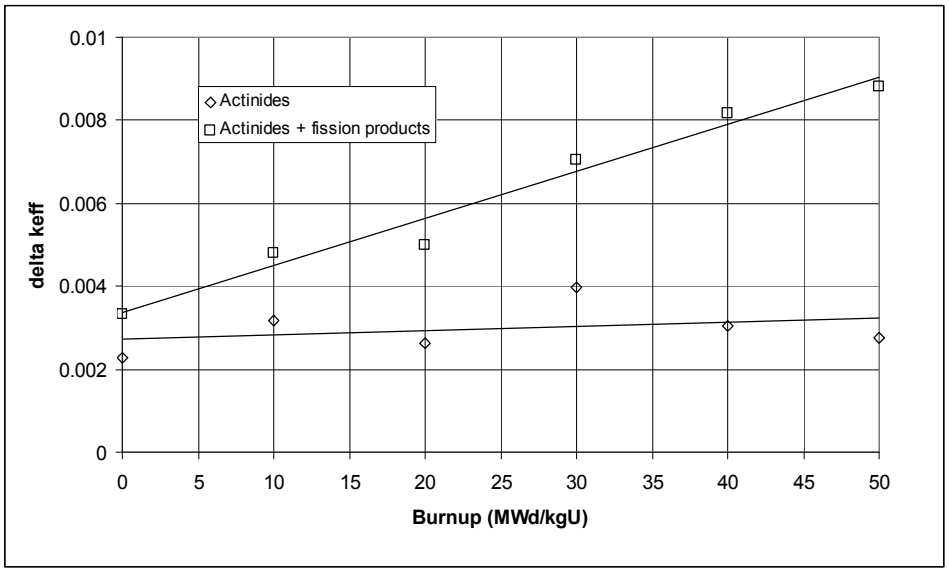

Figure 31 - PWR difference in k_{eff} between calculations with and without nuclide correction factors.

I can be seen for actinides that the calculations with correction factors give a higher k_{eff} of around $\Delta k=0.003$ over the whole burnup range. For actinides + fission products Δk increases from 0.003 at 0 burnup to 0.009 at 50 MWd/kgU.

In /14/ different methods to assess the influence of the spread in the measured/calculated values are presented. Based on the statistical distribution of the values and the standard deviation the Sensitivity/Uncertainty methods were used to assess the uncertainty in k_{eff} due to the spread in the X-values in table 33.

In Sensitivity/Uncertainty method the sensitivity of k_{eff} of variation of the correction factor for each nuclide is calculated. The variation in k_{eff} for each nuclide by changing the correction factor $\pm 2\ \sigma$ vas calculated. The variations in k_{eff} for each nuclide were combined statistically to get the statistical variation on the total k_{eff}. The results are presented in table 34.

Table 34 – PWR k_{eff} in uncertainty calculations (±2σ)

Burnup (MWd/kgU)	Actinides Δk	Actinides and fission products Δk
10	0.0113	0.0143
20	0.0108	0.0138
30	0.0110	0.0140
40	0.0117	0.0147
50	0.0116	0.0146

Adding the values from figure 31 to the uncertainty values in table 34 correction factors for the uncertainty in nuclide calculations are calculated, see table 35. These values are used when developing the loading curve.

Table 35 – PWR correction factors to k_{eff}

Burnup (MWd/kgU)	Actinides Δk	Actinides and fission products Δk
10	0.0162	0.0195
20	0.0158	0.0206
30	0.0194	0.0244
40	0.0210	0.0280
50	0.0220	0.0320

BWR

There are several sets of radiochemical analyses of irradiated fuel samples that could be used to verify the calculations. Isotopes with no measured data are excluded in the analysis.
Measured data have been calculated with the sequence SAS2 /Origen –S report in /15/.

The comparisons are shown in table 36.

Table 36 – BWR comparison between measured and calculated nuclide contents /15/

Nuclide	**No of samples**	**Measured/ computed (average) X**	**Standard-deviation S(X)**
U-234	22	1.002	0.026
U-235	30	1.020	0.034
U-236	30	1.012	0.027
U-238	30	1.001	0.004
Np-237	18	1.011	0.088
Pu-238	30	1.075	0.175
Pu-239	30	1.021	0.061
Pu-240	30	1.009	0.048
Pu-241	30	1.047	0.097
Pu-242	30	0.995	0.125
Am-241	22	0.961	0.110

Note that there are no experimental results for fission products in the BWR-case.

To assess the effect of the results in table 36 the correction factors (X) for all nuclides were used when calculating the k_{eff}. In this case the design case model of a BWR-disposal canister, according to section 6.8 was used.

The results are shown in figure 32.

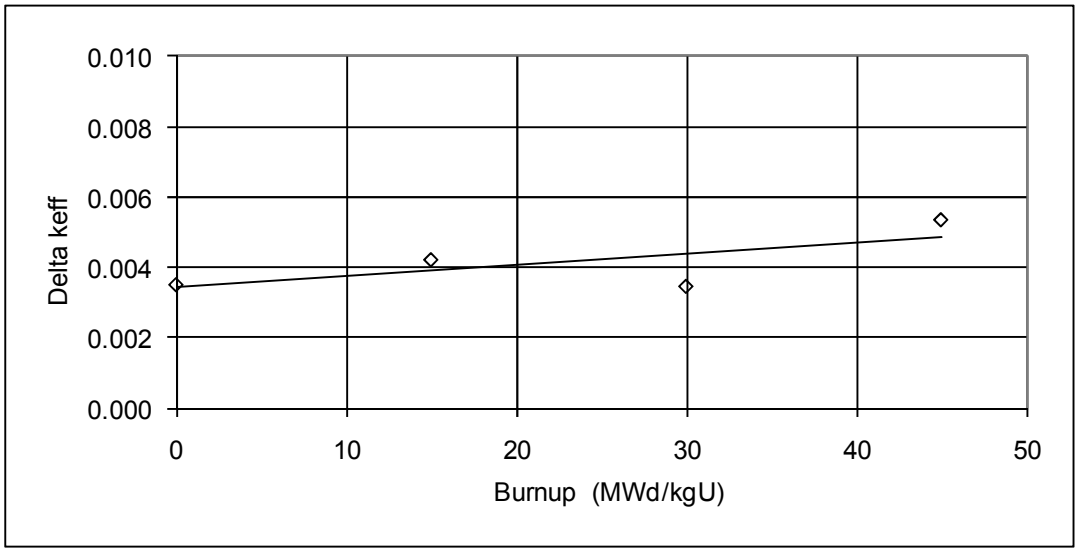

Figure 32 –BWR difference in k_{eff} between calculations with and without nuclide correction factors.

I can be seen for actinides that the calculations with correction factors give a higher k_{eff} of around $\Delta k=0.004$ over the whole burnup range.

In /14/ different methods to assess the influence of the spread in the measured/calculated values are presented. Based on the statistical distribution of the values and the standard deviation the Sensitivity/Uncertainty methods were used to assess the uncertainty in k_{eff} due to the spread in the X-values in table 37.

In Sensitivity/Uncertainty method the sensitivity of k_{eff} of variation of the correction factor for each nuclide is calculated. The variation in k_{eff} for each nuclide by changing the correction factor ±2 σ vas calculated. The variations in k_{eff} for each nuclide were combined statistically to get the statistical variation on the total k_{eff}. The results are presented in table 35.

Table 37 – BWR k_{eff} uncertainty calculations (±2σ)

Burnup (MWd/kgU)	Actinides Δk
15	0.0074
30	0.0105
45	0.0166

Adding the values from figure 32 to the uncertainty values in table 37 correction factors for the uncertainty in nuclide calculations are calculated, see table 38. These values are used when developing the loading curve.

Table 38 – BWR correction factors to k_{eff}

Burnup (MWd/kgU)	Actinides Δk
15	0.0114
30	0.0145
45	0.0206

Since there are no measured data for fission products for BWR the uncertainty factor is estimated for this case.

9.15 Long term reactivity change

Calculations of the long term change of reactivity were done. In this case the design case model of a BWR and a PWR-disposal canister, according to section 6.8 was used. A uniform axial burnup distribution was used.

The results are shown in figure 33 for actinides. It can be seen that the reactivity decreases during the first 100 years, which mainly is due to the decay of fissile Pu-241 with a half life of 14.4 years and buildup of Am-241 and Gd-155 (from Eu-155, half life 4.7 y). After around 100 years the reactivity will increase due to the decay of Am-241 (half life 433 y) and Pu-240 (half life 6560 y). After around 20 000 years the reactivity decreases again after the Am-241- and Pu-240- decay completes and Pu-239 decay dominates. The red line in the figure 33–38 represents the maximum k_{eff}.

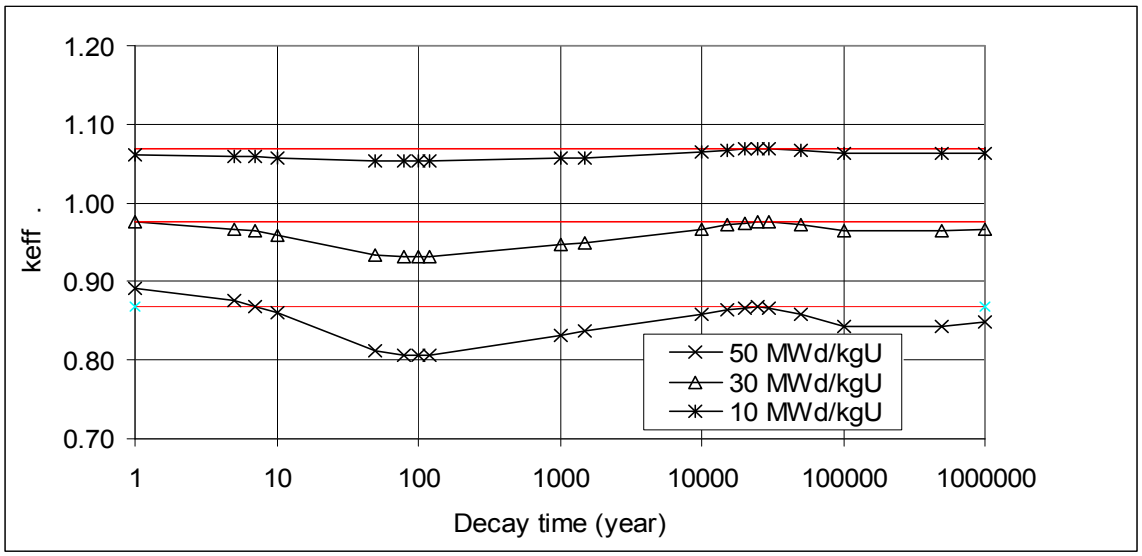

Figure 33 – PWR long term reactivity change for different burnup, actinides (set 1).

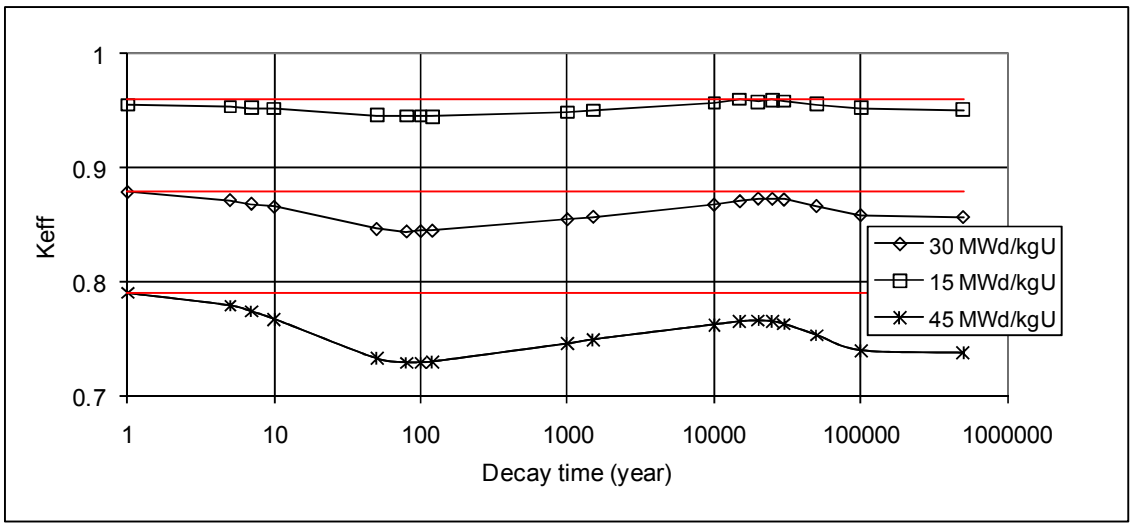

Figure 34 – BWR long term reactivity change for different burnup, actinides (set 1).

Compared to the reactivity level at 1 years decay time the reactivity is always lower than the 1-year value for higher burnup. For lower burnup a correction factor has to be used to account for long term reactivity change. For 10 MWd/kgU a value of $\Delta k_{eff} \pm \sigma$ 0.0080±0.0007 for PWR needs to be used. For BWR $\Delta k_{eff} \pm \sigma$ 0.0048±0.0007 should be used at 15 MWd/kgU.

The results for actinides and fission products (set 2) are shown in figure 35.

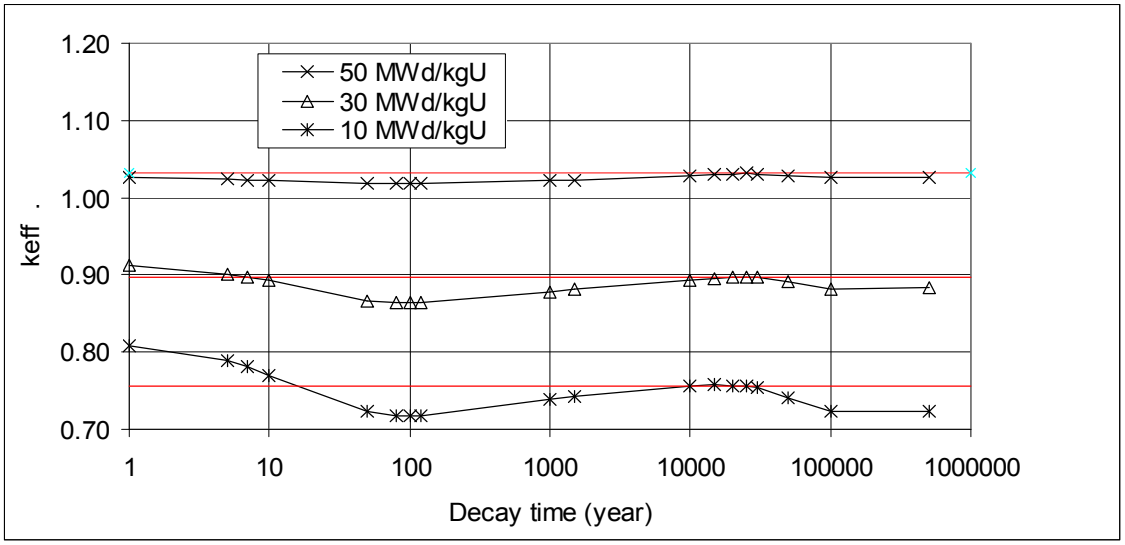

Figure 35 – PWR long term reactivity change for different burnup, actinides and fission products (set 2).

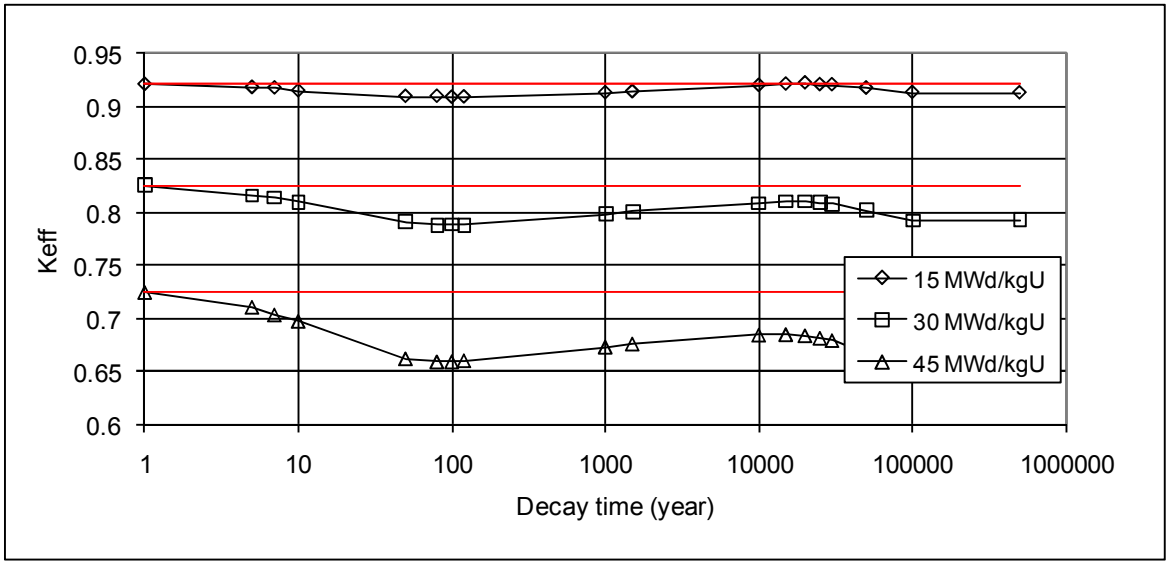

Figure 36 – BWR long term reactivity change for different burnup, actinides and fission products (set 2).

Compared to the reactivity level at 1 years decay time the reactivity is always lower than the 1-year value for all cases. No factor has to be used to account for long term reactivity change for actinides and fission products.

To assess the axial effect (end effect) over long decay times the calculations were repeated with the bounding axial burnup distribution for PWR. In figure 37 the results are shown for actinides (set 1). I the diagram results from the model with uniform axial burnup distribution are compared with results using the bounding axial burnp distribution.

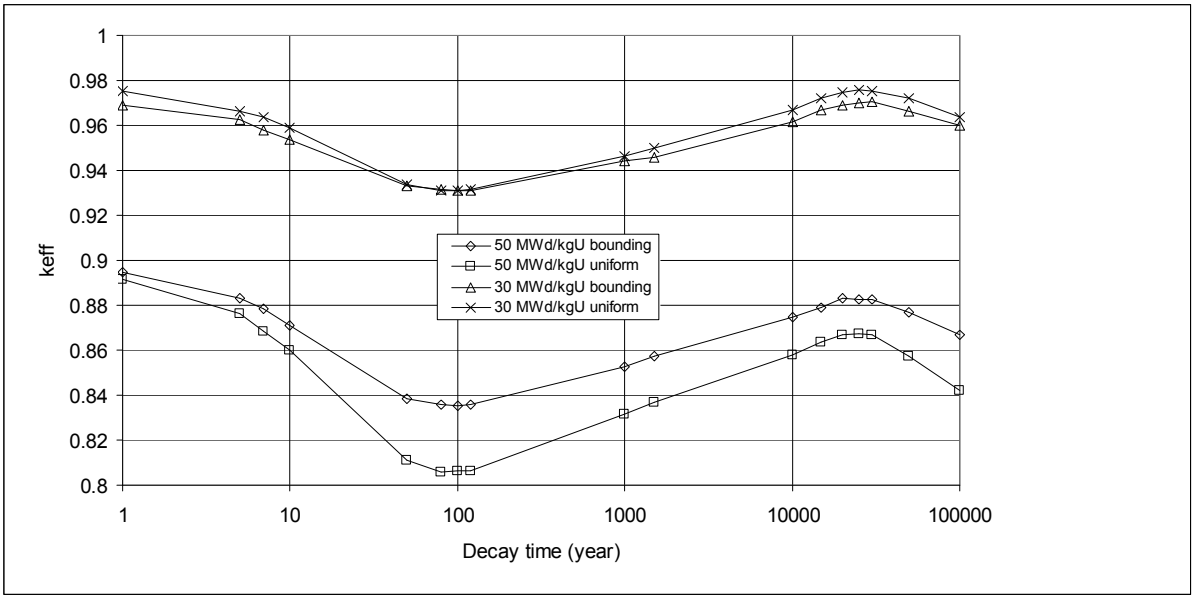

Figure 37 – PWR k_{eff} vs. decay time for bounding and uniform axial burnup distribution, actinides (set 1).

For 30 MWd/kgU the uniform distribution gives higher k_{eff} over all decay times. For 50 MWd/kgU the bounding distribution gives $\Delta k = 0.003$ higher k_{eff} than the uniform distribution at one year decay time. This is consistent with the results of section 9.8. I can also be seen that the relative end effect increases with decay time. The absolute level is always below the 1 year value, so no additional correction factor is needed to account for the decay time dependence of the end effect when developing the loading curve.

In figure 38 the results are shown for actinides and fission products (set 2). I the diagram results from the model with uniform axial burnup distribution are compared with results using the bounding axial burnup distribution.

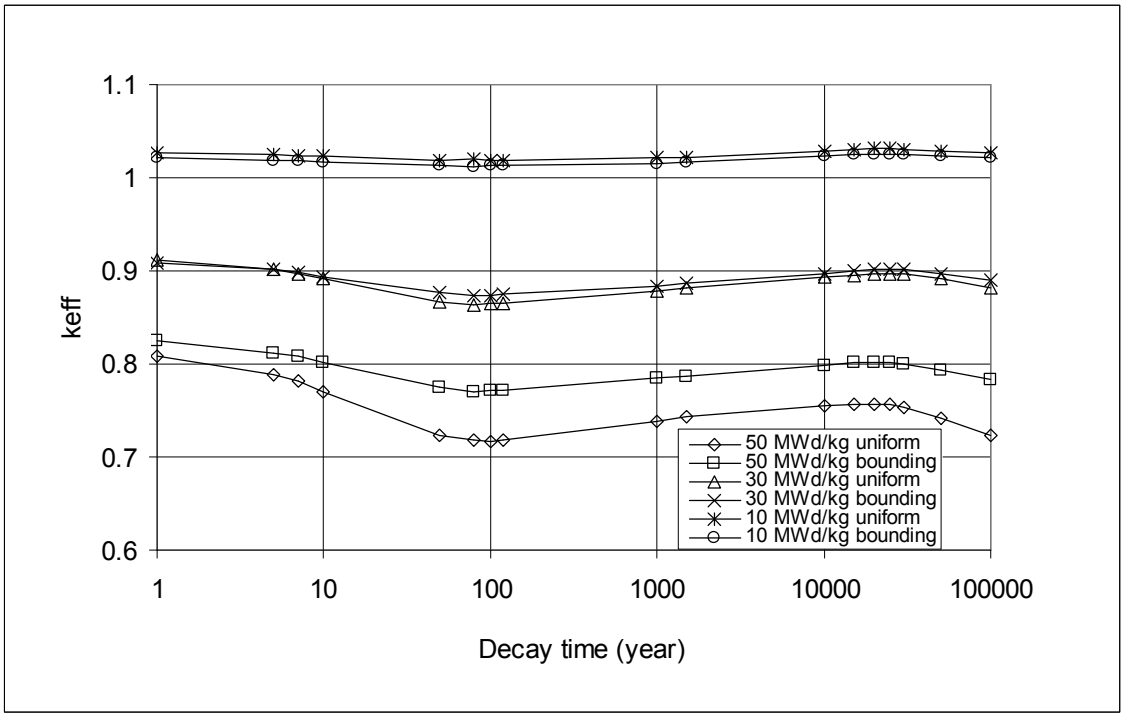

Figure 38 – PWR k_{eff} vs. decay time for bounding and uniform axial burnup distribution, actinides and fission products (set 2).

For 10 MWd/kgU the uniform distribution gives higher k_{eff} over all decay times. For 30 MWd/kgU the bounding distribution gives $\Delta k = 0.001$ lower k_{eff} than the uniform distribution at one year decay time. This is consistent with the results of section 9.8. The end effect will however be positive after 7 years and varies with decay time. The absolute level is always below the one year value, so no additional correction factor is needed to account for the decay time dependence of the end effect when developing the loading curve.

For 50 MWd/kgU the bounding distribution gives $\Delta k = 0.018$ higher k_{eff} than the uniform distribution at one year decay time. This is consistent with the results of section 9.8. I can also be seen that the relative end effect increases with decay time. The absolute level is always below the 1 year value, so no additional correction factor is needed to account for the decay time dependence of the end effect when developing the loading curve.

9.16 Change in geometry due to burnup

The calculations have been done with the assumption that the fuel geometry is nominal. The question is what will happen to the geometry during irradiation. Important measures are the fuel rod outer diameter and the pitch between the fuel rods. A reduction in rod diameter or an increase in fuel rod pitch will increase the reactivity.

The fuel rod pitch is controlled by the spacers and the pitch in the spacers is judged not to change during irradiation. The fuel assembly can, however be bent which could affect the pitch between the spacers. It is judged that bending of a fuel assembly between two spacers not will result in increased pitch.

Results from measurements of the fuel rod diameter on irradiated 17x17 fuel are presented are shown in table 39.

Table 39 - Diameter change due to irradiation

Fuel type	Burnup (MWd/kgU)	Nominal diameter (mm)	Measured (mm)	Reduction (mm)
17x17	62	9.5	9.48	0.02
17x17	60	9.55	9.51	0.04
17x17	57	9.5	9.44	0.06
Svea 100	40	9.62	9.59	0.03

(Source: Hotcelldata utbränt bränsle, Håkan Pettersson, Vattenfall Bränsle 2007.)

It is assumed that 15x15-fuel will be changed in the same way during irradiation. From section 9.13 it can be seen that change in rod diameter gives a reactivity change of -0.0348 Δk/mm. A reduction of the rod diameter of 0.06 mm will the increase the reactivity by $\Delta k = 0.0021$. This value is increased 50% to account for uncertainties in the slope value. $\Delta k_{eff} = 0.0031$ will be used to correct for burnup effects when developing the loading curve.

For BWR change in rod diameter gives a reactivity change of -0.029 Δk/mm. A reduction of the rod diameter of 0.03 mm will the increase the reactivity by $\Delta k = 0.0009$. This value is increased 50% to account for uncertainties in the slope value. $\Delta k_{eff} = 0.0014$ will be used to correct for burnup effects when developing the loading curve.

The active fuel length increases during irradiation. This length increase could be 10–25 mm. In section 9.13 it was shown that changes of this order of magnitude give insignificant reactivity changes.

9.17 Defects in the disposal canister

Different types of defects in the disposal canisters were investigated. Two types of defects were postulated. One was rectangular hole between the central locations in the disposal canister, the other was several circular holes in the disposal canister see figure 39 and 40. In the models the holes are filled with void. Water in the holes will decrease the reactivity.

In the BWR-disposal canister two different defects were simulated:

1. One rectangular hole in the disposal canister with the measures 30x800 mm and a length of 4463 mm.

2. 17 cylindrical holes with a diameter of 20 mm and a length of 4463 mm.

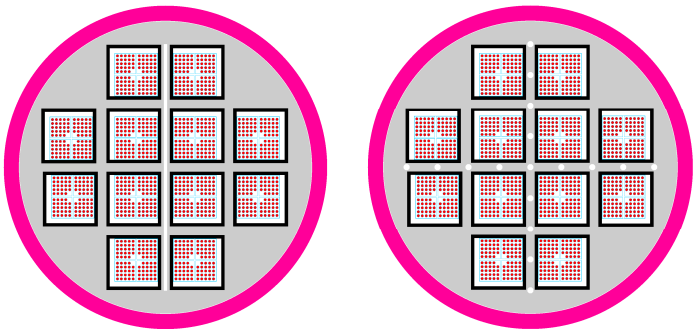

Figure 39 –- BWR disposal canister defects.

In the PWR-disposal canister two different defects were simulated:

1. One rectangular hole in the disposal canister with the measures 30x620 mm and a length of 4443 mm.

2. Nine cylindrical holes with a diameter of 60 mm and a length of 4443 mm.

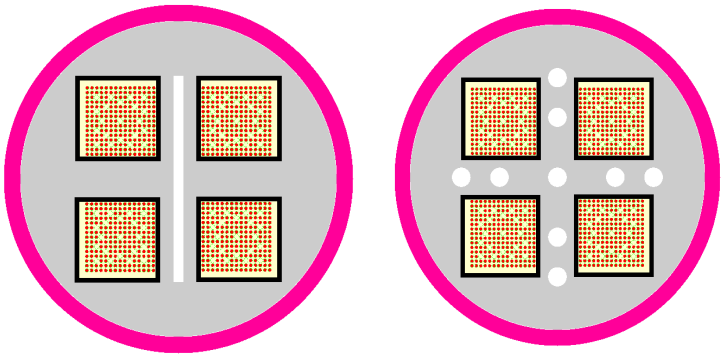

Figure 40 – PWR Disposal canister defects.

The results are shown in table 40.

Table 40 – k_{eff} at different defects in the disposal canister (σ=0.0005)

Case	k_{eff} (σ=±0.0003) BWR	k_{eff} (σ=±0.0003) PWR
Design case	1.0232	1.1041
Rectangular hole in the disposal canister	1.0251	1.1072
Circular holes in the disposal canister	1.0246	1.1063

It can be seen that the defects could increase the reactivity with up to 0.003 Δk.

9.18 Uncertainties in the burnup curve fit

In figures 14 to 17 linear fits to the calculated points were done. The calculated points have a spread around the fitted line which will give an uncertainty in the predicted value if the fitted line is used. This uncertainty is assessed by comparing the difference between calculated values and values predicted by the fitted line. The differences are presented in the table 41.

Table 41 – Calculation of differences and uncertainty factors

BWR

Burnup	Actinides								
	5.0 % U-235			4.5 % U-235			4.0 % U-235		
MWd/kgU	Calculated valus	Predicted value	Difference	Calculated valus	Predicted value	Difference	Calculated valus	Predicted value	Difference
15	0.9580	0.9523	-0.0057	0.9306	0.9234	-0.0073	0.8995	0.8922	-0.0073
30	0.8816	0.8755	-0.0061	0.8467	0.8415	-0.0052	0.8081	0.8044	-0.0036
45	0.7926	0.7986	0.0060	0.7537	0.7597	0.0060	0.7118	0.7167	0.0049
Root of sum of squares			0.0103			0.0107			0.0095
Burnup	Actinides and fissionproducts								
	5.0 % U-235			4.5 % U-235			4.0 % U-235		
MWd/kgU	Calculated valus	Predicted value	Difference	Calculated valus	Predicted value	Difference	Calculated valus	Predicted value	Difference
15	0.9231	0.9243	0.0012	0.8959	0.8957	-0.0002	0.8639	0.8646	0.0007
30	0.8272	0.8258	-0.0014	0.7932	0.7925	-0.0008	0.7546	0.7563	0.0017
45	0.7268	0.7273	0.0005	0.6887	0.6893	0.0006	0.6493	0.6480	-0.0013
Root of sum of squares			0.0019			0.0010			0.0023

PWR

Burnup	Actinides								
	5.0 % U-235			4.5 % U-235			4.0 % U-235		
MWd/kgU	Calculated valus	Predicted value	Difference	Calculated valus	Predicted value	Difference	Calculated valus	Predicted value	Difference
15	0.9580	0.9523	-0.0057	0.9306	0.9234	-0.0073	0.8995	0.8922	-0.0073
30	0.8816	0.8755	-0.0061	0.8467	0.8415	-0.0052	0.8081	0.8044	-0.0036
45	0.7926	0.7986	0.0060	0.7537	0.7597	0.0060	0.7118	0.7167	0.0049
Root of sum of squares			0.0103			0.0107			0.0095
Burnup	Actinides and fissionproducts								
	5.0 % U- 235			4.5 % U-235			4.0 % U-235		
MWd/kgU	Calculated valus	Predicted value	Difference	Calculated valus	Predicted value	Difference	Calculated valus	Predicted value	Difference
15	0.9231	0.9243	0.0012	0.8959	0.8957	-0.0002	0.8639	0.8646	0.0007
30	0.8272	0.8258	-0.0014	0.7932	0.7925	-0.0008	0.7546	0.7563	0.0017
45	0.7268	0.7273	0.0005	0.6887	0.6893	0.0006	0.6493	0.6480	-0.0013
Root of sum of squares			0.0019			0.0010			0.0023

The roots of the sum of the squares of the differences of the k_{eff} are used as uncertainty factors in the loading curve.

10 Loading curve

PWR

Based on the cases calculated for different initial enrichments, the burnup dependence and the uncertainties factors a loading curve was developed. All factors are shown in tables 42 and 43.

Table 42 – Burnup requirements for different enrichments, PWR

	Actinides			**Actinides and fissionsproducts**		
Enrichment	**5.0**	**4.0**	**3.0**	**5.0**	**4.0**	**3.0**
Uncertainties						
Uncertainties in fuel data	0.0028	0.0028	0.0028	0.0028	0.0028	0.0028
Uncertainties in burnup curve fit	0.0009	0.0054	0.0061	0.0128	0.0175	0.0169
Statistical uncertainty in KENO	0.0009	0.0009	0.0009	0.0009	0.0009	0.0009
Bias in benchmarking	0.0007	0.0007	0.0007	0.0007	0.0007	0.0007
Calculational uncertainty	0.0093	0.0093	0.0093	0.0093	0.0093	0.0093
Uncertainty and bias in nuclide calculation	0.0224	0.0200	0.0174	0.0279	0.0249	0.0208
Uncertainty in burnup	0.0078	0.0060	0.0036	0.0083	0.0066	0.0040
End effect	0.0032	0.0000	0.0000	0.0000	0.0000	0.0000
Horizontal burnup distribution	0.0045	0.0025	0.0012	0.0039	0.0028	0.0015
Long term effect	0.0000	0.0000	0.0037	0.0000	0.0000	0.0028
Defects in the cansister	0.0030	0.0030	0.0030	0.0030	0.0030	0.0030
Change in geometry due to burnup	0.0031	0.0031	0.0031	0.0031	0.0031	0.0031
Sum	0.0586	0.0536	0.0516	0.0727	0.0715	0.0658
k_{eff} in base case	1.1041	1.0594	0.9951	1.1041	1.0594	0.9951
Sum k_{eff}	1.1627	1.1130	1.0467	1.1768	1.1309	1.0609
Limit vaule	0.9500	0.9500	0.9500	0.9500	0.9500	0.9500
Need of BU-cred	0.2127	0.1630	0.0967	0.2268	0.1809	0.1109
Bu coefficient (dk/MWd/kgU)	0.0042	0.0044	0.0046	0.0058	0.0060	0.0064
Burnup requirement (MWd/kgU)	**51.1**	**36.8**	**20.9**	**39.3**	**30.0**	**17.3**

On the bottom line the burnup requirement for different enrichments are seen.

Table 43 – Burnup requirements for different enrichments, BWR

	Actinides			Actinides and fissionsproducts		
Enrichment	**5.0**	**4.5**	**4.0**	**5.0**	**4.5**	**4.0**
Uncertainties						
Uncertainties in fuel data	0.0020	0.0020	0.0020	0.0020	0.0020	0.0020
Uncertainties in burnup curve fit	0.0103	0.0107	0.0095	0.0019	0.0010	0.0023
Statistical uncertainty in KENO	0.0009	0.0009	0.0009	0.0009	0.0009	0.0009
Bias in benchmarking	0.0007	0.0007	0.0007	0.0007	0.0007	0.0007
Calculational uncertainty	0.0093	0.0093	0.0093	0.0093	0.0093	0.0093
Uncertainty and bias in nuclide calculation	0.0151	0.0120	0.0100	0.0197	0.0104	0.0088
Uncertainty in burnup	0.0062	0.0038	0.0028	0.0058	0.0036	0.0024
End effect	0.0207	0.0032	0.0000	0.0233	0.0069	0.0017
Horizontal burnup distribution	0.0018	0.0017	0.0012	0.0029	0.0020	0.0010
Long term effect	0.0005	0.0037	0.0058	0.0007	0.0015	0.0019
Defects in the disposal canister	0.0030	0.0030	0.0030	0.0030	0.0030	0.0030
Change in geometry due to burnup	0.0014	0.0014	0.0014	0.0014	0.0014	0.0014
Sum	0.0719	0.0524	0.0466	0.0715	0.0427	0.0354
k_{eff} in base case	1.0232	0.99854	0.97388	1.0232	0.99854	0.97388
Sum k_{eff}	1.0951	1.0510	1.0204	1.0947	1.0412	1.0093
Limit vaule	0.9500	0.9500	0.9500	0.9500	0.9500	0.9500
Need of BU-cred	0.1451	0.1010	0.0704	0.1447	0.0912	0.0593
Bu coefficient (dk/MWd/kgU)	0.0051	0.0055	0.0059	0.0066	0.0069	0.0072
Burnup requirement (MWd/kgU)	**28.3**	**18.4**	**12.0**	**22.0**	**13.3**	**8.2**

Based on the information in tables 42 and 43 loading curves can be developed. A loading curve combines all the points of initial enrichments and burnup requirements that will produce k_{eff}=0.95 in the disposal canister including uncertainties. The loading curves are shown in figure 42. If the assembly initial enrichment/burnup is on the right side of the curve, the assembly is accepted to be loaded in a disposal canister. The loading curves cover all fuel types analyzed in section 6.2.

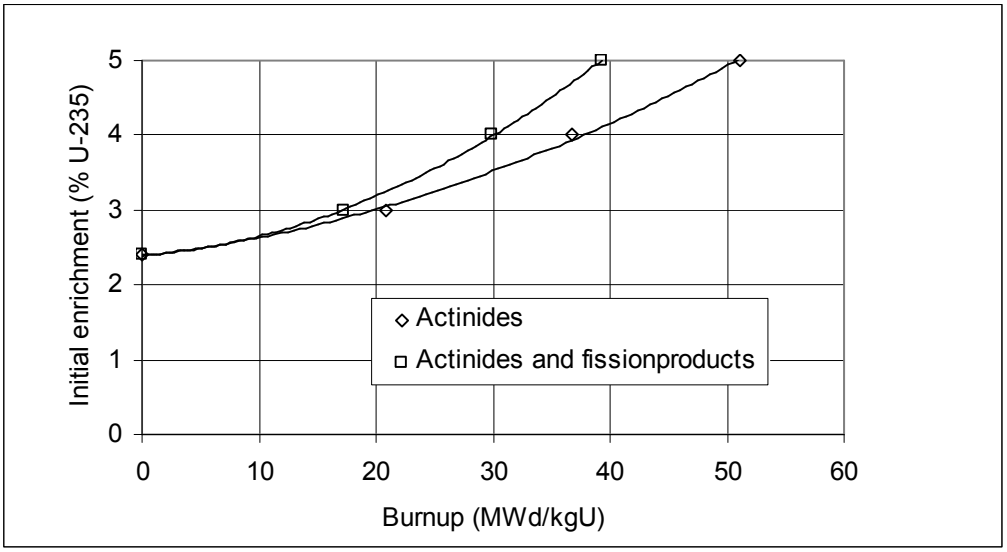

Figure 42 – Loading curve for the disposal canister, PWR-fuel.

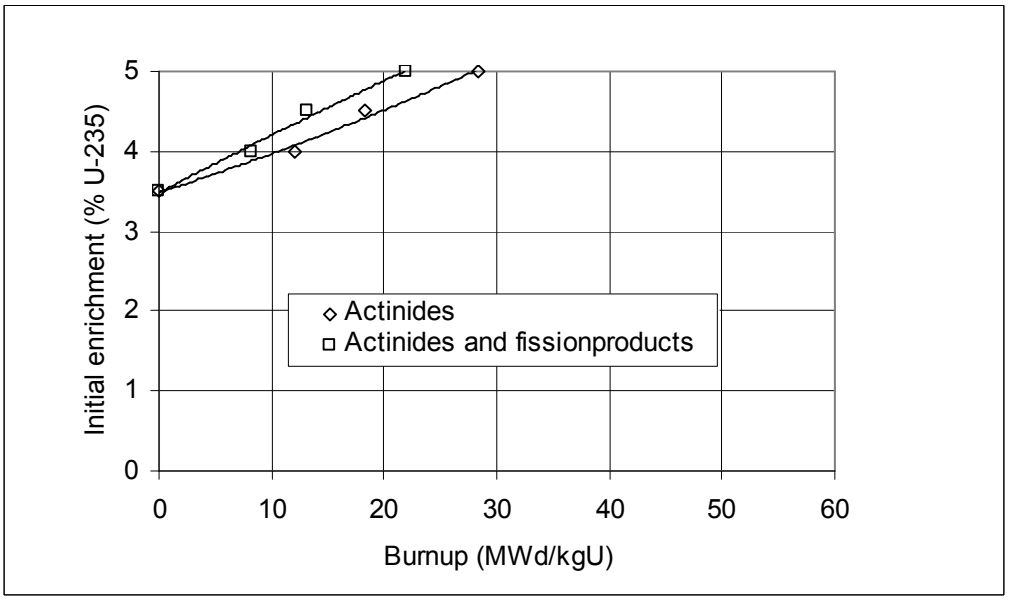

Figure 43 – Loading curve for the disposal canister, BWR-fuel.

It should be noted that the maximum enrichment should be used to check the criteria, which is the value used should contain margin for manufacturing tolerances in enrichment. The burnup value should be the best estimate assembly average burnup.

In the figure 44 all PWR fuel assemblies (2517 assemblies) stored in Clab at end of 2007 are plotted (combinations of initial enrichment and average assembly burnup). Each assembly is represented by a ×.

In the same diagram the loading curves are shown. The fuel assemblies that appear on the right side of the limit curves will result in a $k_{eff} < 0.95$. It can be seen that all PWR-assemblies except three stored in Clab at the end of 2007 could be accepted for storage in disposal canisters for final storage using burnup credit for actinides only (set 1). Using set 2, actinides and fission products the margin increases and all assemblies meet the criteria.

For future fuel the burnup target for 4.6% enriched fuel is 53–58 MWd/kgU depending on reactor, which gives an acceptable margin to the set 1 loading curve.

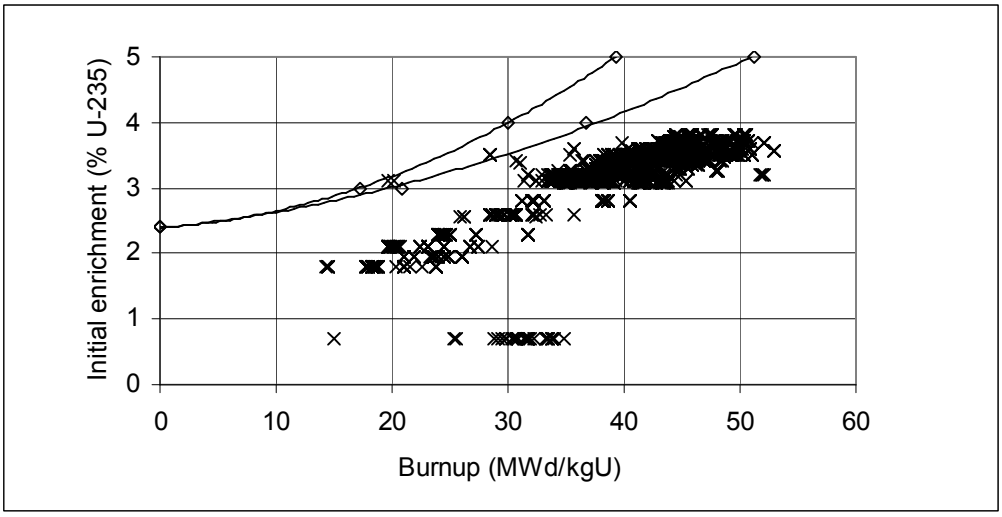

Figure 44 – Loading curves for PWR compared to the Clab-inventory 2007-12-31.

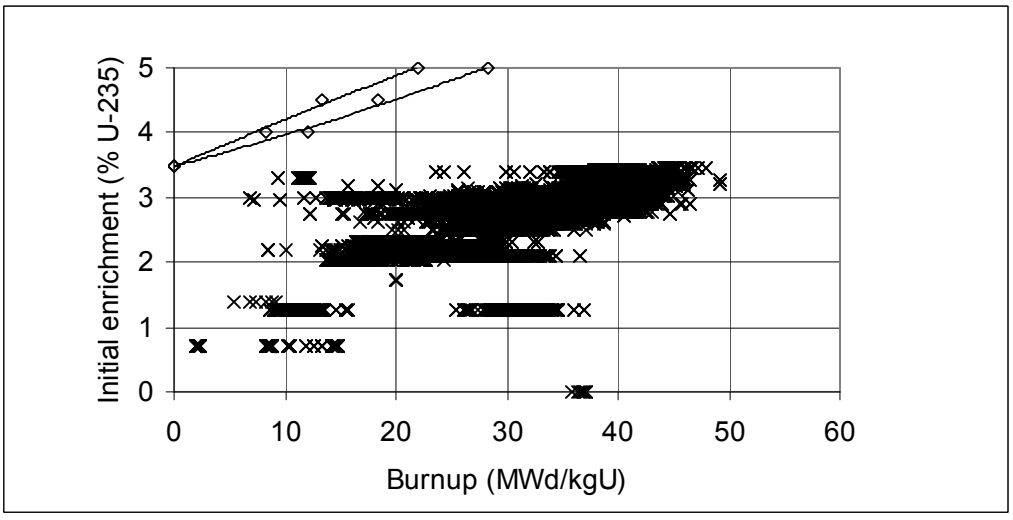

Figure 45 – Loading curves for BWR compared to the Clab-inventory 2007-12-31.

11 Conclusions

This study, based on state of the art methods and an assessment of the uncertainties, shows that burnup credit is an acceptable way to control the reactivity in the disposal canisters using a minimum set of nuclides, actinides only (set 1). If selected fission products also are credited (set 2) more margin is achieved.

For assemblies that not meet the criteria in the loading curve the number of assemblies in the disposal canister can be reduced in order to reduce the reactivity. Another possibility is to combine the fuel assembly that does not meet the criteria with fuel assemblies with lower enrichment and high burnup. In this case specific analyses have to be performed.

For the BWR- case fresh fuel with 5% U-235 enrichment can be loaded in the disposal canister if two central compartments are blocked, that is the number of fuel assemblies is reduced from 12 to 10.

For the PWR-case fresh fuel with enrichments up to 3.5% U-235 can be loaded with sufficient margin to the criticality limit assuming only one assembly in the disposal canister. For enrichments above 3.5% U-235 burnup has to be credited. For 5% enriched fuel a burnup of 21 MWd/kgU is needed if actinides are credited and 15 MWd/kgU if actinides + fission products are credited assuming one assembly in the disposal canister. If the unlikely event occurs that some fuel assemblies will not meet these requirements special arrangements have to be developed, e.g. special material in the insert or reconstruction of the fuel assemblies. Fuel assemblies that have contained burnable poison rods have to be analyzed separately.

12 References

SKB´s (Svensk Kärnbränslehantering AB) publications can be found at www.skb.se/publications. References to SKB´s unpublished documents are listed separately at the end of the reference list. Unpublished documents will be submitted upon request to document@skb.se.

1. **Agrenius Ingenjörsbyrå AB, 1999.** Kriticitetsförhållanden i kapslar för slutförvaring av använt kärnbränsle. SKB R-99-52, Svensk Kärnbränslehantering AB.

2. **Agrenius L, 2002.** Criticality safety calculations of storage canisters. SKB TR-02-17, Svensk Kärnbränslehantering AB.

3. Scale: A Modular Code System for Performing Standardized Computer Analyses, ORNL/TM-2005/39.

4. **Pers K, Leskinen N, Ronneteg U, Cederqvist L, Johansson M,** Design, production and initial state of the canister. SKB TR-10-14, Svensk Kärnbränslehantering AB.

5. SKB Inkapsling Projekt PM 96-3430-06, Kriticitetsberäkningar och parameterstudier för slutförvarskapsel med insats, april 1996.

6. Review and Prioritization of Technical Issues Related to Burnup Credit for LWR Fuel, Oak Ridge Laboratory, US Nuclear Regulatory Commission, NUREG/CR -6665, February 2000.

7. Parametric Analysis of PWR Spent Fuel Depletion Parameters for Long Term Disposal Criticality Safety, ORNL/TM – 1999/99.

8. Study of the effect of integral burnable absorbers for PWR burnup credit, NUREG/CR-6760, March 2003, Oak Ridge National Laboratory.

9. Parametric study of the effect of burnable poison rods PWR burnup credit, NUREG/CR-6761, March 2002, Oak Ridge National Laboratory.

10. Recommendations for addressing axial burnup distributions in PWR burnup credit analyis, NUREG/CR-6801, October 2002, Oak Ridge National Laboratory.

11. Sandia Corporation, SCR-607, Factors for one-sided tolerance limits and for variable sampling plans, D B Owen, March 1963.

12. Validation of the Scale System For PWR Spent Fuel Isotopic Composition Analyses, ORNL/TM-12667.

13. An extension of the Validation of the Scale (SAS2) Isotopic Predictions for PWR Spent Fuel, ORNL/TM 13317.

14. Strategies for application of Isotopic Uncertainties in Burnup Credit, NUREG/CR-6811, June 2003.

15. Validation of the Scale (SAS2H) Isotopic Predictions for BWR Spent Fuel, ORNL/TM- 13315.

Unpublished documents

SKBdoc id	version	Title	Issuer, year
1251579	1.0	Faktablad – Berggrundens uppbyggnad. Geologivägen i Västernorrland, 2007.	SKB, 2010

13 Appendices

Appendix 1 – Calculations of criticality experiments

Case no	Case designation	Enrichment (%U235)	Description	Calculated k_{eff}	Standard deviation
1	p2438x05	2.35	No absorber plates	0.9978	0.0016
2	p2438x17	2.35	Boral absorber plates	0.9973	0.0010
3	p2438x28	2.35	Stainless steel absorber plates	0.9957	0.0016
4	p2615x14	4.31	Stainless steel absorber plates	0.9976	0.0017
5	p2615x23	4.31	Cadmium absorber plates	1.0006	0.0017
6	p2615x31	4.31	Boral absorber plates	1.0010	0.0016
7	p2827u2a	2.35	Uranium reflector	1.0020	0.0014
8	p2827l2a	2.35	Lead reflector	0.9994	0.0015
9	p2827non	2.35	No reflector	0.9953	0.0015
10	p2827u2b	4.31	Uranium reflector	1.0008	0.0016
11	p2827l2b	4.31	Lead reflector	1.0098	0.0009
12	p3314a	4.31	0.226 cm Boroflex absorber plates	1.0021	0.0015
13	p3314b	4.31	0.452 cm Boroflex absorber plates	1.0014	0.0013
14	p3602n2	2.35	Steel reflector. no absorber	1.0036	0.0013
15	p3602non	4.31	Steel reflector. no absorber	1.0060	0.0017
16	p3602s4	4.31	Steel reflector. borated steel absorber plates	1.0030	0.0014
17	p3602b4	4.31	Steel reflector. Boral absorber plates	1.0042	0.0016
18	p3602c4	4.31	Steel reflector. cadmium absorber plates	1.0038	0.0012
19	p3926u2a	2.35	Uranium reflector	0.9983	0.0017
20	p3926l2a	2.35	Lead reflector	1.0011	0.0014
21	p3926n2	2.35	No reflector	0.9924	0.0018
22	p3926u4a	4.31	Uranium reflector	0.9998	0.0019
23	p3926l4a	4.31	Lead reflector	1.0047	0.0019
24	p3926nob	4.31	No reflector	0.9997	0.0016
25	p4267a	4.31	No soluble boron	0.9964	0.0011
26	p4267b	4.31	2550 ppm soluble boron	1.0008	0.0013
27	p4267c	4.31	No soluble boron	0.9978	0.0012
28	p4267d	4.31	2550 ppm soluble boron	0.9951	0.0016
29	pnl194	4.31	Hexagonal lattice. narrow pitch	1.0050	0.0017
30	ft214r	4.31	Flux traps. no voids	0.9935	0.0016
31	ft214v3	4.31	Flux traps with voids	0.9956	0.0011
32	bawl231a	4	Core I - 1152 ppm soluble borom	0.9945	0.0010
33	bawl231b	4	Core I - 3389 ppm soluble borom	0.9972	0.0009
34	bawl273m	2.46	Core XX - 1675 ppm soluble boron	0.9974	0.0014
35	bawl484a	2.46	Core IV - 84 B4C pins	0.9930	0.0011
36	bawl484b	2.46	Core IX - No B4C pins	0.9933	0.0016
37	bawl484c	2.46	Core XIII - 1.6 wt% Boral	0.9963	0.0019
38	bawl484d	2.46	Core XXI - 0.1 wt% Boral	0.9900	0.0017
39	bawl645t	2.46	Triangular pitch. pitch = pin O.D.	1.0055	0.0010
40	bawl645s	2.46	Square pitch. pitch = pin O.D.	1.0026	0.0012
41	bwl645so	2.46	Square pitch. pitch = 1.17*pin O.D.	1.0018	0.0012
42	bnwl810a	2.46/4.02	Core 12 - No Gd fuel rods	0.9985	0.0015
43	bnwl810b	2.46/4.02	Core 14 - 12 Gd fuel rods	0.9973	0.0016
44	bnwl810c	2.46/4.02	Core 16 - 16 Gd fuel rods	0.9981	0.0014
45	e196u6n	2.35	0.615 in. pitch. 0 ppm soluble boron	0.9951	0.0017
46	epru615b	2.35	0.615 in. pitch. 464 ppm soluble boron	0.9970	0.0013
47	epru75	2.35	0.750 in. pitch. 0 ppm soluble boron	0.9968	0.0011
48	epru75b	2.35	0.750 in. pitch. 568 ppm soluble boron	1.0005	0.0010
49	e196u87c	2.35	0.870 in. pitch. 0 ppm soluble boron	0.9961	0.0016
50	epru87b	2.35	0.870 in. pitch. 286 ppm soluble boron	0.9971	0.0016
51	saxu56	5.74	2 lattice pitches. SS clad. 0.56 in. pitch	0.9906	0.0018
52	saxu792	5.74	2 lattice pitches. SS clad. 0.792 in. pitch	0.9967	0.0012
53	w3269a	3.7	Ag-In-Cd (0.330 in. O.D) absorber rods	1.0031	0.0010
54	w3269b	3.7	Ag-In-Cd (0.330 in. O.D) absorber rods	1.0035	0.0015
55	w3269c	2.72	Ag-In-Cd (0.403 in. O.D) absorber rods	0.9933	0.0010
56	ans33bp2	4.75	Cruciform box. polyethylene	1.0001	0.0012
57	ans33bb2	4.75	Cruciform box. polyethylene	1.0089	0.0011
58	ans33bh2	4.75	Cruciform box only	1.0134	0.0011
59	ans33h2	4.75	No absorbers	0.9990	0.0014
Average				0.9993	
Standard deviation				0.0046	
K(59)				2.0260	
95%/95% LTL				0.0094	
Bias				0.0007	

Main parameters for the BWR fuel assemblies

Appendix 2

Parameter	Fuel type																		
	AA 8x8	Exxon 8x8	KWU 8x8-2	ANF 9x9-5	KWU 9x9-5	KWU 9x9-Q	Atrium 9A	Atrium 10B	Atrium 10 XM	GE11S	GE12S	GE14	GNF2	Svea 64	Svea 100	Svea 96	Svea 96 Optima	Svea 96 Optima 2	Svea96 Optima 3
	1	**1**	**1**	**1**	**1**	**1**	**2**	**2**	**3**	**2**	**2**	**5**	**4**	**6**	**7**	**8**	**9**	**10**	**11**
Niumber of fuel rods	64	63	62	76	76	72	72	91	91	74	91	92	92	64	100	96	96	96	96
Fuel rod pitch, medel (mm)	15.8/16.05/16.3	16.26	16.25	14.53	14.45	14.45	14.45	12.95	12.95	14.38	12.95	12.95	12.95	15.8	12.7	12.7	12.6-12.75	12.78	12.77
Fuel rod outer diameter (mm)	12.25	12.34	12.3	10.59	11	11	11	10.05	10.28	11.18	10.26	10.26	10.26	12.25	9.62	9.62	10.3/9.62	9.84	9.84
Fuel rod inner diameter (mm)	10.65	10.66	10.66	9.11	9.66	9.66	9.67	8.84	9.054	9.76	8.98	8.94	9.06	10.65	8.36	8.36	8.94/8.36	8.63	8.63
Cladding thickness (mm)	0.8	0.84	0.82	0.74	0.67	0.67	0.665	0.605	0.613	0.71	0.64	0.66	0.6	0.8	0.63	0.63	0.68/0.63	0.605	0.61
Cladding material	Zr2	Zr2	Zr2	Zr2	Zr2	Zr2	Zr2	Zr2	Zr2	Zr2	Zr2	Zr2	Zr2	Zr2	Zr4	Zr2	Zr2	Zr2	Zr2
Pellet diameter (mm)	10.44	10.26	10.44	8.93	9.5	9.5	9.5	8.67	8.87	9.55	8.81	8.76	8.88	10.44	8.19	8.19	8.77/8.19	8.48	8.48
UO2 density (g/cc)	10.41	10.5	10.45	10.36	10.45	10.45	10.55	10.55	10.6	10.56	10.56	10.5	10.53	10.5	10.5	10.5	10.52	10.6	10.60
Active fuel length (mm)	3712	3720	3680	3712	3680	3680	3680	3680	3690	3690	3690	3680	3680	3680	3750	3600	3710	3710	3690
Nunber of water rods		1	2	5	5	9	9	9	9	17	9	8	8	0	0	4	4	4	4
Water rod outer diameter (mm)		12.34	15	14.02	13.15					24.9	24.9	24.9	24.9						
Water rod inner diameter (mm)		10.66	13.4	13.42	11.59					23.38	23.38	23.38	23.38						
Water rod cladding thickness (mm)		0.84	0.8	0.3	0.78					0.76	0.76	0.76	0.76						
Channel outer measures (mm)	138.6	138.6	138.6	138.6	138.6	138.6	138.6	138.6	138.6	137.36	137.36	137.36	137.5	139.6	139.6	139.6	139.6	140.2	140.2
Channel inner measures (mm)	134	134	134	134	134	134	134	134	134	134.06	134.06	134.06	134.2	137.4	137.4	137.4	137.4	137.4	137.4
Channel wall thickness (mm)	2.3	2.3	2.3	2.3	2.3	2.3	2.3	2.3	2.3	1.65	1.65	1.65	1.65	1.1	1.1	1.1	1.1	1.4	1.4
Channel material	Zr	Zr	Zr	Zr	Zr	Zr	Zr	Zr	Zr	Zr	Zr	Zr	Zr	Zr	Zr	Zr	Zr	Zr	Zr
Central cross inner width (mm)														5.6	29.7	29.7	29.6	29.6	29.60
Central cross wall thickness (mm)														0.8	0.8	0.8	0.8	0.8	0.8
Central channel outer measures (mm)																			
Central channel outer measures (mm)							37.05x37.05	35x 35	35x35										
Central channel wall thickness							0.725	0.725	0.8										
Central channel material							Zr	Zr	Zr										

Source

1. Clab96 – Dataunderlag för kriticitetsberäkningar, Agrenius Ingenjörsbyrå AB, augusti 1991
2. PB - 82-99 - Vattenfall- Clab - Verifikationa av kriticitetssäkerheten vid förvaring av nya bränsleyper
3. AiC-1334697-1 Data for final storag for lead test assemblies for Ringhals 1
4. 2006 R21D Forsmark 3 GNF2
5. 2008 R23E Forsmark 3 GE14
6. BK 91-705 Svea 64 för Ringhals 1 - Mekanisk konstruktion
7. BK 90-205, ABB Atom Svea-100 med 12.7 mm stavdelning för Oskarshamn 3
8. BLB 00-050 - Mekaniskt datablad för nukleär och termohydraulisk design O1 e24 (Svea 96S Optima/L)
9. BLB 98-122, rev 1 - Mekaniskt datablad för nukleär och termohydraulisk design B1 e23 och B2 e19 Demo (Svea 96S Optima)
10. BTK 00-144, rev 2 Mekaniskt datablad för nukleär och termohydraulisk design SVEA-96 Optima 2 i Oskarshamn 3
11. BTK 04-246, rev 1 Mekaniskt datablad för nukleär och termohydraulisk design O3 e21 Svea 96 Optima3

Main parameters for the PWR fuel assemblies

Appendix 3

Parameter	Fuel type											
	W15x15	KWU15x15	F15*15AFA3G	15x15AGORA	W17x17	AA17*17	F17*17	S17*17HTP	17x17 HTTP	17x17 HTP M5	17x17 HTP M5 Monobloc	17x17 AFA3G
Reference	1	1	2	3	1	1	9	4	5	6	7	10
Numbler of fuel rods	204	204	204	204	264	264	264	264	264	264	264	264
Fuel rod pitch (mm)	14.3	14.3	14.3	14.3	12.6	12.6	12.6	12.6	12.6	12.6	12.6	12.6
Fuel rod outer diameter (mm)	10.72	10.75	10.72	10.77	9.5	9.5	9.5	9.55	9.55	9.5	9.5	9.5
Fuel rod inner diameter (mm)	9.48	9.3	9.484	9.505	8.36	8.36	8.36	8.33	8.33	8.36	8.36	8.36
Cladding thickness (mm)	0.62	0.725	0.618	0.6325	0.57	0.57	0.57	0.61	0.61	0.57	0.57	0.57
Pellet diameter (mm)	9.20	9.11	9.294	9.33	8.19	8.19	8.19	8.17	8.165	8.192	8.192	8.192
Cladding material	Zr4	Zr4	M5	M5	Zr4	Zr4	Zr4	Zr4	Zr4	M5	M5	M5
Active length (mm)	3658	3658	3658	3658	3658	3658	3658	3658	3658	3658	3658	3658
Density UO2 (g/cc)	10.22	10.46	10.52	10.52	10.45	10.45	10.45	10.45	10.45	10.52	10.55	10.52
Number of guide tubes	20	20	20	20	24	24	24	24	24	24	24	24
Material in guide tube	Zr4	Zr4	M5	M5	Zr4	Zr4	Zr4	PCAm	PCAm	PCAm	PCAm	Zr4
Guide tube outer diameter (mm)	13.87	13.86	14.1	14.1	12.24	12.09	12.05	12.24	12.24	12.24	12.45	12.45
Guide tube inner diameter (mm)	13.01	13	13.05	13.05	11.44	11.18	11.25	11.3	11.3	11.3	11.45	11.45
Guide tube cladding thickness	0.43	0.43	0.525	0.525	0.4	0.455	0.4	0.47	0.47	0.47	0.5	0.5
Number of instrument tubes	1	1	1	1	1	1	1	1	1	1	1	1
Material in instrument tube	Zr4	Zr4	M5	M5	Zr4	Zr4	Zr4	PCAm	PCAm	PCAm	PCAm	Zr4
Instrument tube outer diameter (mm)	13.87	13.86	14.1	14.1	12.24	12.09	12.05	12.24	12.24	12.24	12.45	12.45
Instrument tube inner diameter (mm)	13.01	13	13.05	13.05	11.44	11.18	11.25	11.3	11.3	11.3	11.45	11.45
Instrument tube cladding thickness	0.43	0.43	0.525	0.525	0.4	0.455	0.4	0.47	0.47	0.47	0.5	0.5

Source. 1. CLAB 96 - Dataunderlag för kriticitetsberäkningar, Agrenius Ingenjörsbyrå AB, augusti 1991
2. Areva FF DC 02916 Transport and reprocessing document for raeload SSPK od Rinfhals 2 fuel assemblies 15x15AFA3GAA
3. Areva A1C-1332397-0 NP fuel assemblies delivered to Ringhals 2/31/07
4. Fuel type data for final storage - PWR - Siemens HTTP Ringhals 3 2000-06-16
5. Areva A1C-1313665-4 Reprocessing information for Framatom ANP fule assemblies delivered to delivered to Ringhals 3/4
6. Areva A1C-1333871-0 NP fuel assemblies delivered to RH 3/25/08
7. Areva A1C-133864-0 NP fuel assemblies delivered to RH 3/24/07
8. Fuel type data for final storage - PWR - reload 18 / SUPW Ringhals 4
9. ABB BR 91-446 Criticality calculations: PWR Compact canisters (Clab 96), 1991-10-28
10. Fuel Typa Data for Final Storage - PWR - Reload 18 / SUPW Ringhals 4 17x17AFA3

Data for axial distributions **Appendix 4**

Reactor	Cycle id									No if fuel assemblies in core	No of axial distributions
O1	eoc30	eoc 31	eoc 32	eoc 33	eoc 34					448	2240
O2	eoc30	eoc 31	eoc 32	eoc 33	eoc 34					444	2220
O3	eoc22	eoc 25	eoc 26	eoc 27	eoc 28					700	3500
F1	eco24b	eoc25	eoc26	eoc 27	eoc28					676	3380
F2	eoc23	eoc24	eoc25	eoc26	eoc27					676	3380
F3	eoc20	eoc21	eoc22	eoc24	eoc25					700	3500
R1	eoc28	eoc29	eoc30	eoc31	eoc32					648	3240
No of BWR distributions											21460
R2	eoc29	eoc30	eoc31	eoc32	eoc33					157	785
R3	eoc22	eoc23	eoc24	eoc25	eoc26					157	785
R4	eoc22	eoc23	eoc24	eoc25	eoc26					157	785
R3 Great	c1	c2	c3	c5	c5	c6	c7	c8	c9	157	1413
R4 Frej	c1	c2	c3	c5	c5	c6	c7	c8a	c8b	157	1413
No of PWR distributions											5181

(Source: Previous references 23–25 to this document. Link in SKBdoc.)